HyperMu: Laser spectroscopy of 1S HFS in muonic Hydrogen

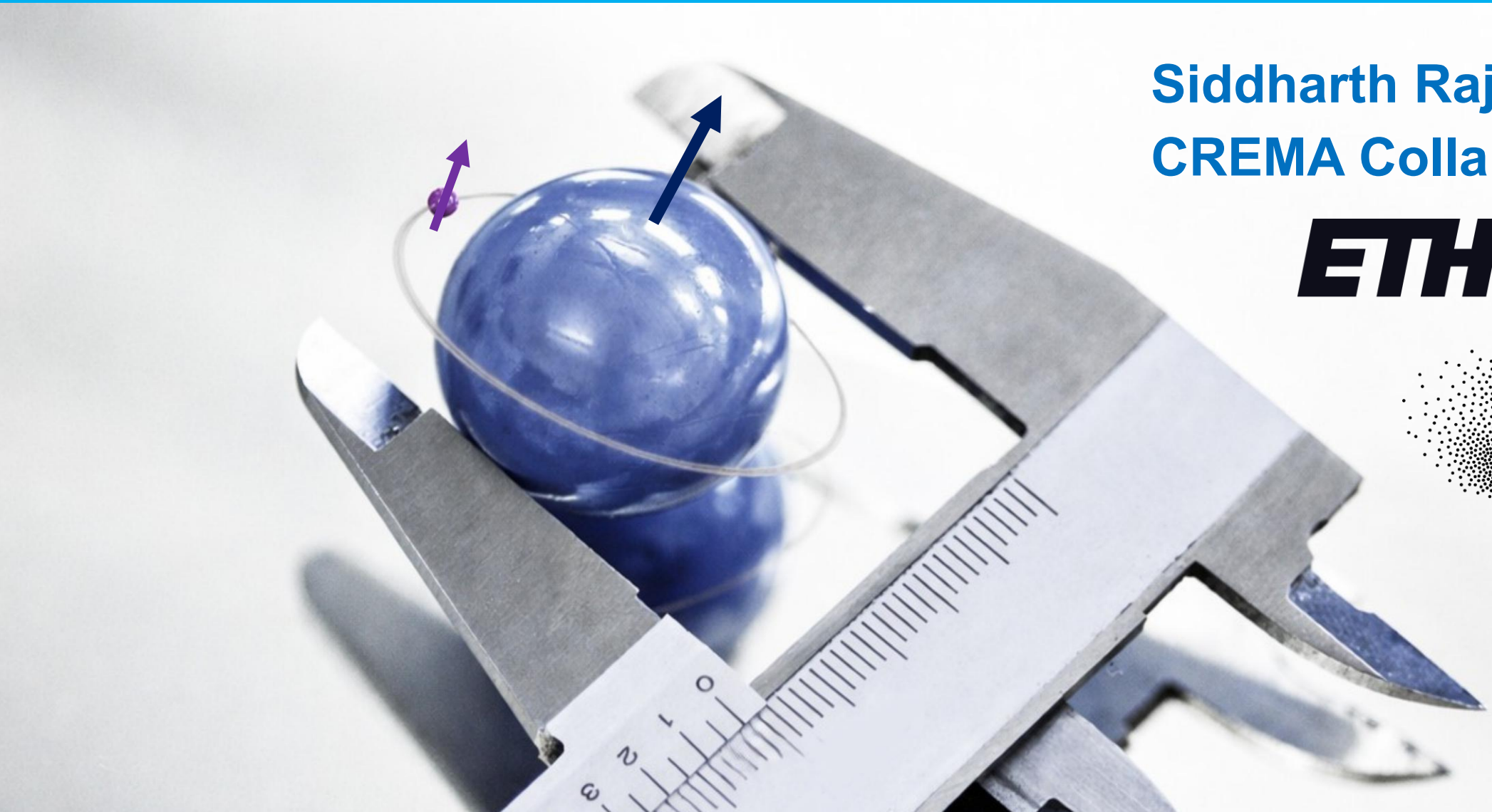

Siddharth Rajamohanan
CREMA Collaboration

ETH zürich

PSI

PSAS 2026

Muonic hydrogen

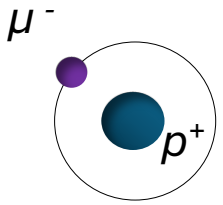

$$\Rightarrow \mu^- \xrightarrow[2.2\,\mu s]{} e^- + \bar{\nu}_e + \nu_\mu$$

$$\Rightarrow m_\mu \approx 207\, m_e$$

$$\Rightarrow E_n \approx -\frac{R_\infty}{n^2}\frac{m_l}{m_e}$$

$$\Rightarrow \delta E_{\mathrm{fns}} \propto |\Psi(0)|^2 \propto m_l^3$$

$$\Rightarrow \text{small systematics, large sensitivity}$$

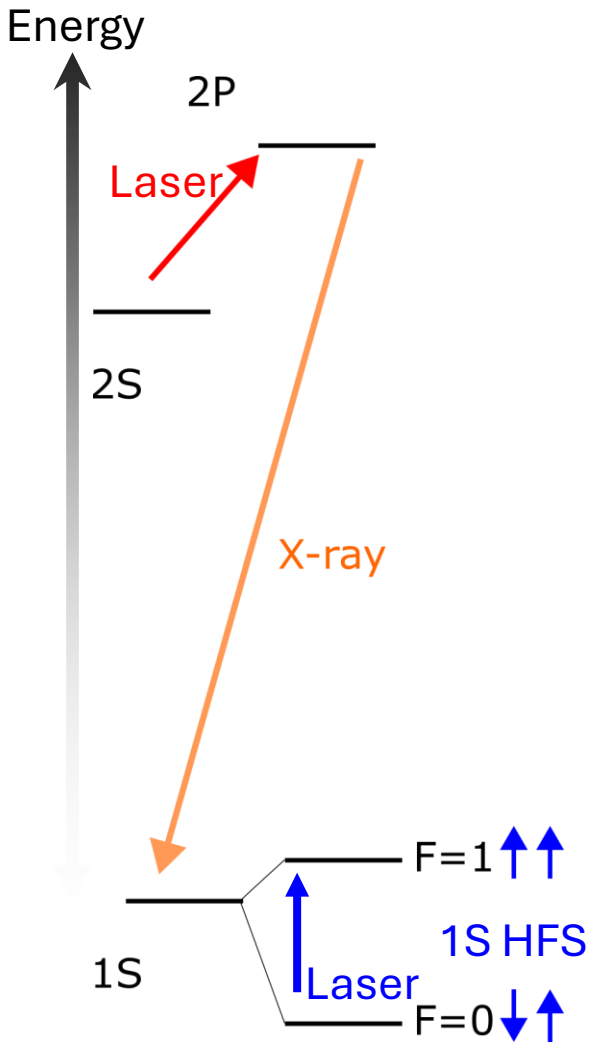

Proton's Electric Charge Radius

$$\mathrm{R_p} \equiv -\frac{6}{\mathrm{G_E}(0)}\frac{\mathrm{dG_E}}{\mathrm{dQ^2}}\bigg|_{\mathrm{Q^2=0}}$$

Pohl et al, Nature 466, 2010

Proton's Zemach Radius

$$\mathrm{R_Z} \equiv \frac{4}{\pi}\int_0^\infty \frac{\mathrm{dQ}}{\mathrm{Q^2}}\left[1 - \mathrm{G_E}(-\mathrm{Q^2})\frac{\mathrm{G_M}(-\mathrm{Q^2})}{1+\kappa_\mathrm{P}}\right]$$

Recent theory improvements

$$E_{hfs}^{1S} = E_F(1 + \delta_{QED} + \delta_{hVP} + \underbrace{\delta_{fns} + \delta_{rec} + \delta_{pol}}_{\text{Two photon exchange}} + \dots)$$

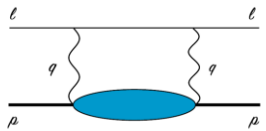

+ . . .

Recent theory improvements

$$E_{hfs}^{1S} = E_F(\,1 + \delta_{QED} + \delta_{hVP} + \underbrace{\delta_{fns} + \delta_{rec} + \delta_{pol}}_{\text{Two photon exchange}} + \dots\,)$$

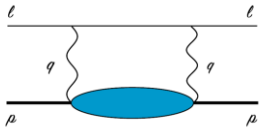

+ . . .

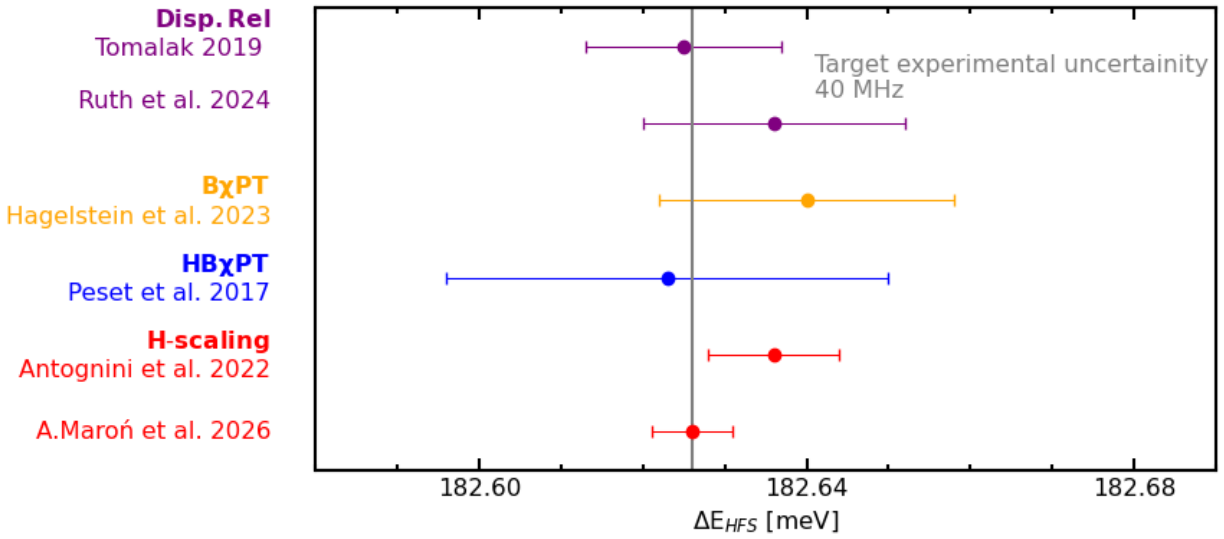

Recent theory improvements

$$E_{hfs}^{1S} = E_F(1 + \delta_{QED} + \delta_{hVP} + \underbrace{\delta_{fns} + \delta_{rec} + \delta_{pol}}_{\text{Two photon exchange}} + \dots)$$

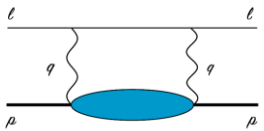

+ . . .

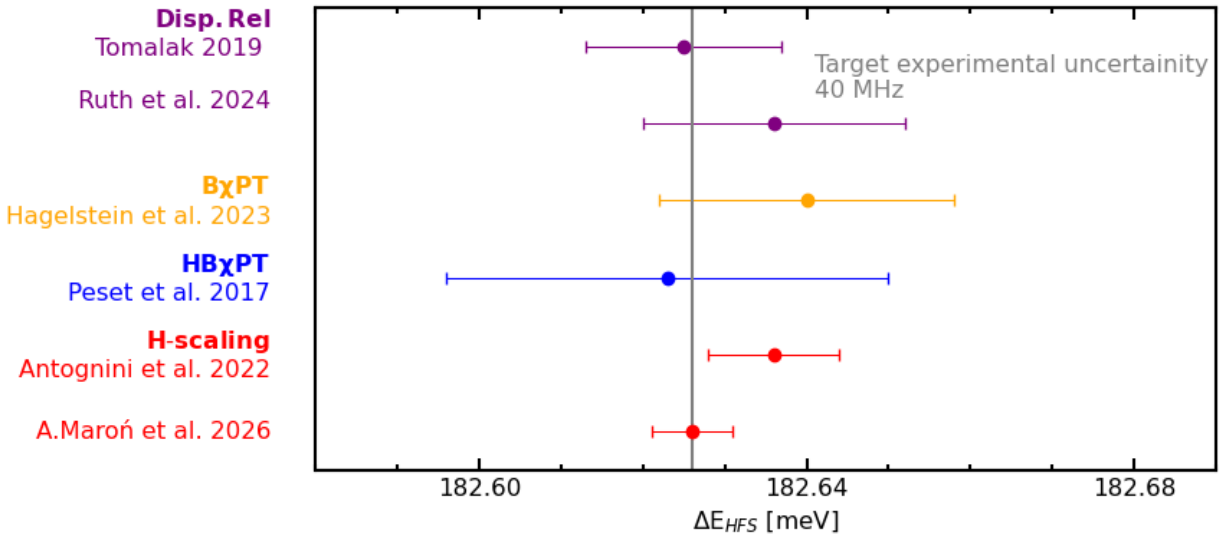

Term	Value
a_μ	0.001 165 92
$(1+a_\mu)\,\delta^{(1)}_{evp}$	0.006 082 37
$(1+a_\mu)\,\delta^{(2)}_{evp}$	0.000 061 32
$\delta^{(2)}$	−0.000 016 34
$\delta^{(3)}$	−0.000 007 10
$\delta^{(3)}_{rel,evp}$	0.000 001 15
$\delta^{(3)}_{\mu vp,evp}$	0.000 001 17
$\delta^{(3)}_{se,evp1}$	−0.000 001 70
$\delta^{(3)}_{se,evp2}$	0.000 000(2)
Lin, Meißner, Hammer (2022) $\delta^{(1)}_{fns}$	−0.008 237(21)
Antognini , Lin, Meißner (2022) $\delta^{(1)}_{rec}$	0.001 672(3)
Ruth et al. (2024) $\delta^{(1)}_{pol}$	0.000 200 6(52 4)
$\frac{\alpha}{\pi}\,c_1\,\delta^{(1)}_{fns}$	−0.000 033 12
$\frac{\alpha}{\pi}\,c_1\,\delta^{(1)}_{rec}$	0.000 006 72
$\delta^{(2)}_{evp,fns}$	−0.000 149 81
$\delta^{(2)}_{evp,rec}$	0.000 025 24
$\delta^{(2)}_{\mu vp,fns}$	−0.000 025 10
$\delta^{(2)}_{\mu vp,rec}$	−0.000 001 18
$\delta^{(2)}_{se,fns}$	0.000 016 18
$\delta^{(2)}_{se,rec}$	0.000 016 48
$\delta^{(2)}_{rel,fns}$	−0.000 050 85
$\delta^{(2)}_{rel,rec}$	0.000 118 86
$\delta^{(2)}_{rel,rec2}$	0.000 000(12)
$\delta^{(2)}_{rel,rec,fns}$	0.000 000(12)
$\delta^{(2)}_{hvp}$	0.000 011 80(8)
$\delta^{(3)}_{fns}$	0.000 000(2)
δ_{weak}	0.000 011 99
δ	0.000 870 (60)
$\frac{m_\mu}{m_e}\,[\delta_{exp}(H) - \delta(H)]$	0.000 133
δ_{corr}	0.001 003 (30)

Maroń, Pańtak, Pachucki 2026
arXiv:2604.06930

Recent theory improvements

$$\mathrm{E}_{\mathrm{hfs}}^{1\mathrm{S}} = \mathrm{E}_{\mathrm{F}}\left(\, 1 + \delta_{\mathrm{QED}} + \delta_{\mathrm{hVP}} + \underbrace{\delta_{\mathrm{fns}} + \delta_{\mathrm{rec}} + \delta_{\mathrm{pol}}}_{\text{Two photon exchange}} + \ldots \right)$$

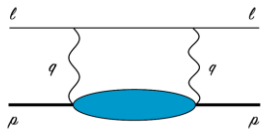

+ . . .

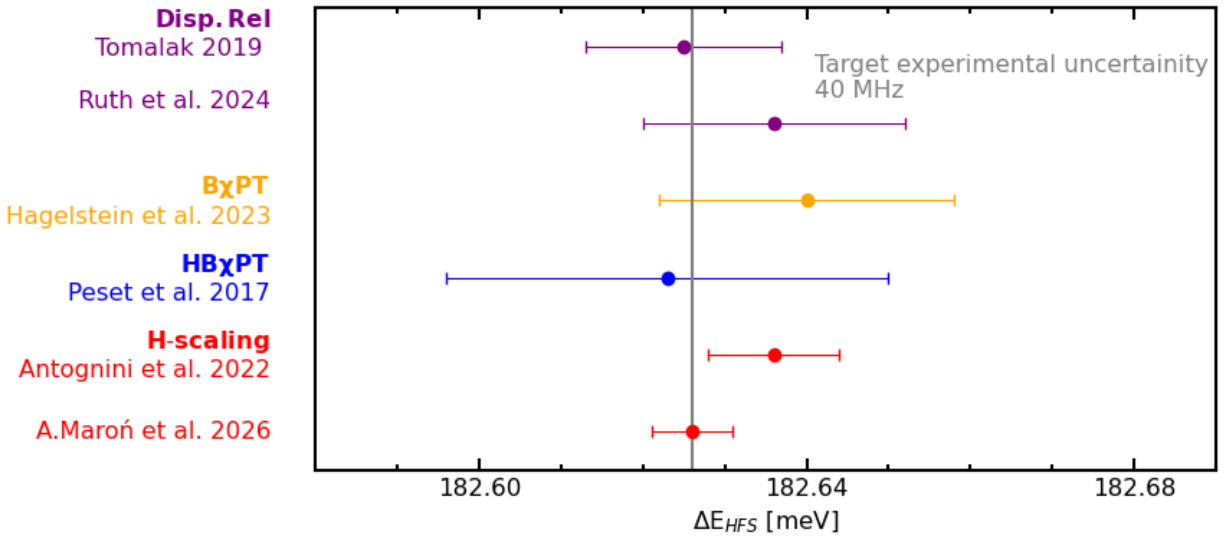

$$\begin{aligned}
\mathrm{E}_{\mathrm{hfs}}(\mu H) = \mathrm{E}_{\mathrm{F}}\,(1 + \delta_{\mathrm{corr}}) &= 0.182\,626(5)\ \mathrm{eV} \\
&\hat{=} 6.788\,97(19)\ \mu\mathrm{m} \\
&\hat{=} 44.158\,8(12)\ \mathrm{THz} \\
\text{Our goal} &= 44.15?\ ???(40)\ \mathrm{THz} \qquad [1\mathrm{ppm}]
\end{aligned}$$

Term	Value
a_μ	0.001 165 92
$(1+a_\mu)\,\delta^{(1)}_{\mathrm{evp}}$	0.006 082 37
$(1+a_\mu)\,\delta^{(2)}_{\mathrm{evp}}$	0.000 061 32
$\delta^{(2)}$	−0.000 016 34
$\delta^{(3)}$	−0.000 007 10
$\delta^{(3)}_{\mathrm{rel,evp}}$	0.000 001 15
$\delta^{(3)}_{\mu\mathrm{vp,evp}}$	0.000 001 17
$\delta^{(3)}_{\mathrm{se,evp1}}$	−0.000 001 70
$\delta^{(3)}_{\mathrm{se,evp2}}$	0.000 000(2)
Lin, Meißner, Hammer (2022) $\delta^{(1)}_{\mathrm{fns}}$	−0.008 237(21)
Antognini , Lin, Meißner (2022) $\delta^{(1)}_{\mathrm{rec}}$	0.001 672(3)
Ruth et al. (2024) $\delta^{(1)}_{\mathrm{pol}}$	0.000 200 6(52 4)
$\frac{\alpha}{\pi}\,c_1\,\delta^{(1)}_{\mathrm{fns}}$	−0.000 033 12
$\frac{\alpha}{\pi}\,c_1\,\delta^{(1)}_{\mathrm{rec}}$	0.000 006 72
$\delta^{(2)}_{\mathrm{evp,fns}}$	−0.000 149 81
$\delta^{(2)}_{\mathrm{evp,rec}}$	0.000 025 24
$\delta^{(2)}_{\mu\mathrm{vp,fns}}$	−0.000 025 10
$\delta^{(2)}_{\mu\mathrm{vp,rec}}$	−0.000 001 18
$\delta^{(2)}_{\mathrm{se,fns}}$	0.000 016 18
$\delta^{(2)}_{\mathrm{se,rec}}$	0.000 016 48
$\delta^{(2)}_{\mathrm{rel,fns}}$	−0.000 050 85
$\delta^{(2)}_{\mathrm{rel,rec}}$	0.000 118 86
$\delta^{(2)}_{\mathrm{rel,rec2}}$	0.000 000(12)
$\delta^{(2)}_{\mathrm{rel,rec,fns}}$	0.000 000(12)
$\delta^{(2)}_{\mathrm{hvp}}$	0.000 011 80(8)
$\delta^{(3)}_{\mathrm{fns}}$	0.000 000(2)
δ_{weak}	0.000 011 99
δ	0.000 870 (60)
$\frac{m_\mu}{m_e}\,[\delta_{\mathrm{exp}}(\mathrm{H}) - \delta(\mathrm{H})]$	0.000 133
δ_{corr}	0.001 003 (30)

Maroń, Pańtak, Pachucki 2026
arXiv:2604.06930

HyperMu experiment at PSI

HyperMu experiment at PSI

590 MeV proton beam on graphite target → π^- → μ^-

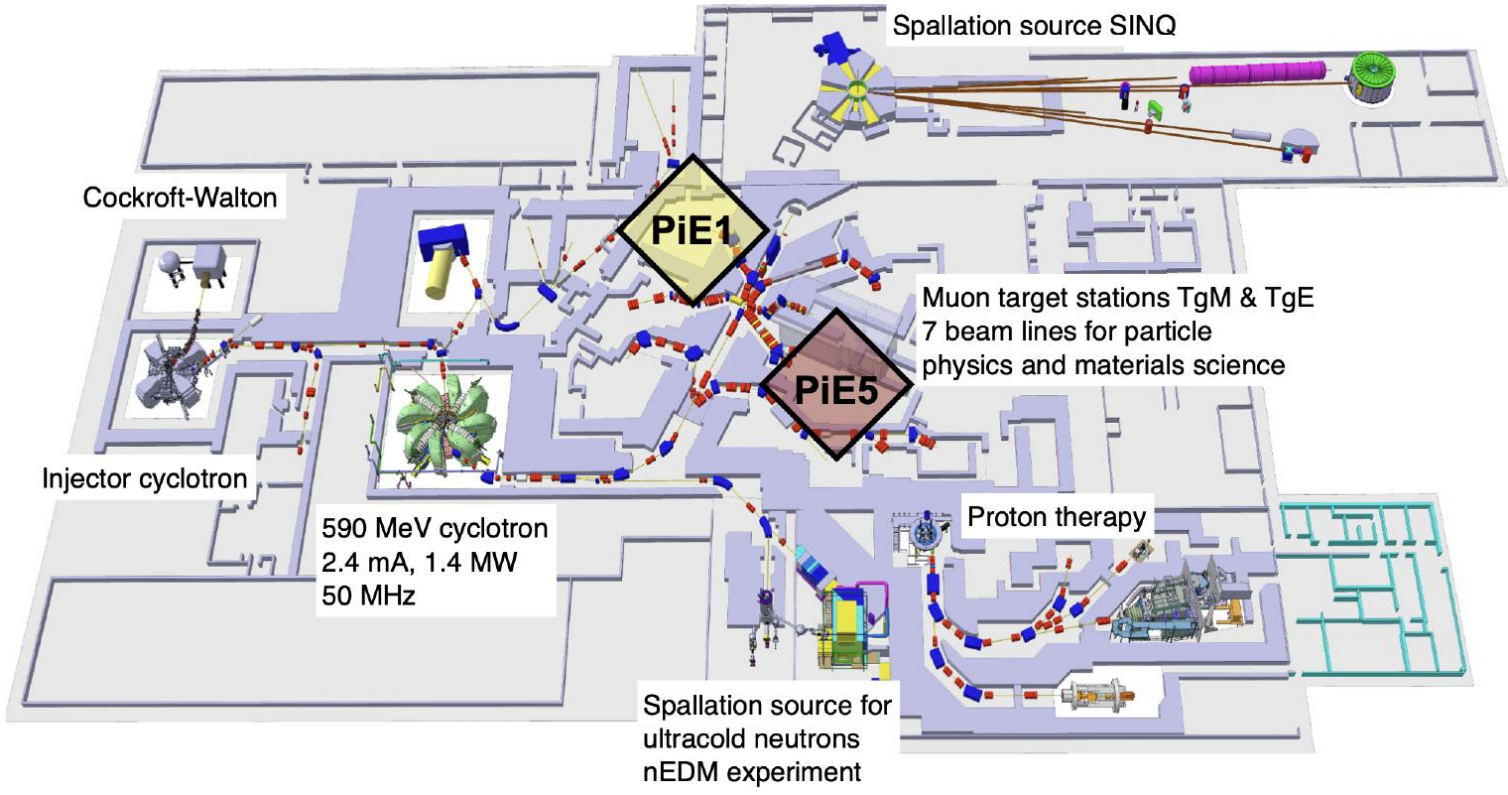

HyperMu experiment at PSI

590 MeV proton beam on graphite target → π^- → μ^-

PiE5 continuous μ^- beamline
- Rate ~ 2000 /s
- Momentum ~ 12 MeV/c

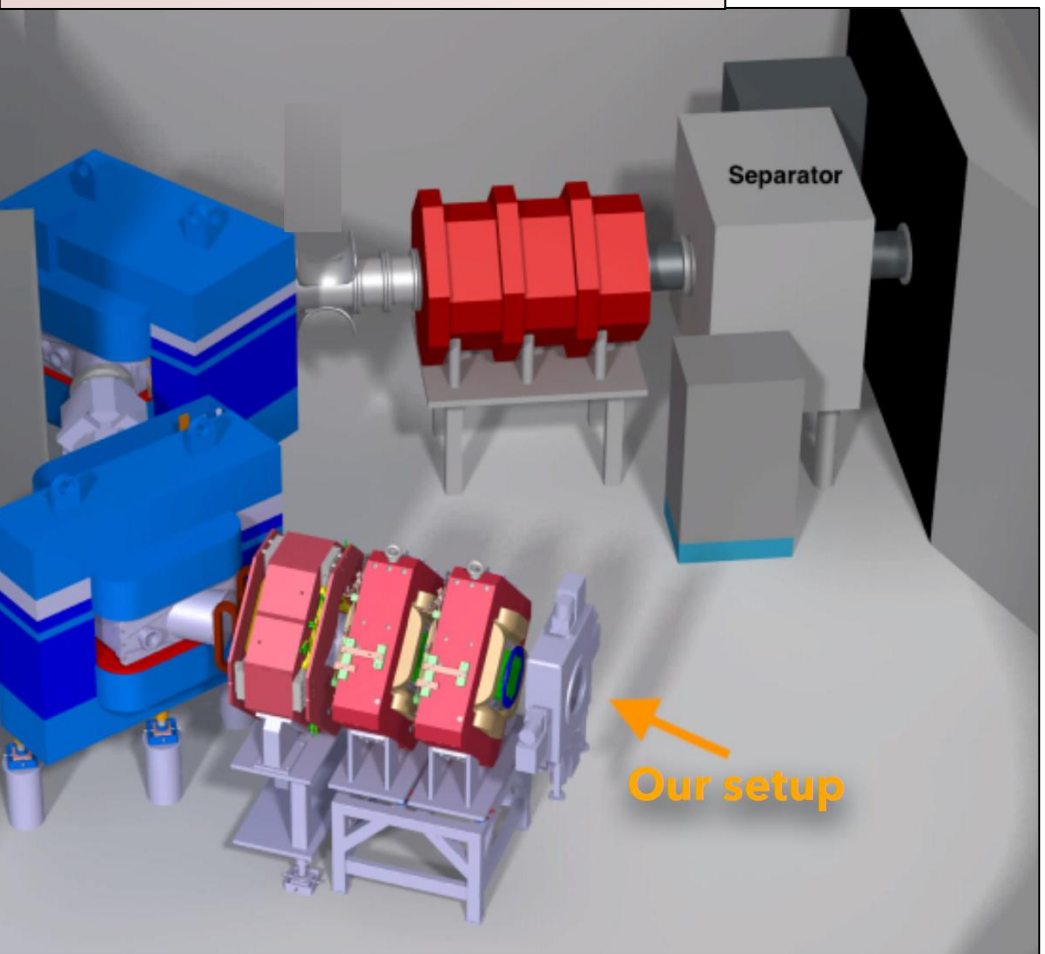

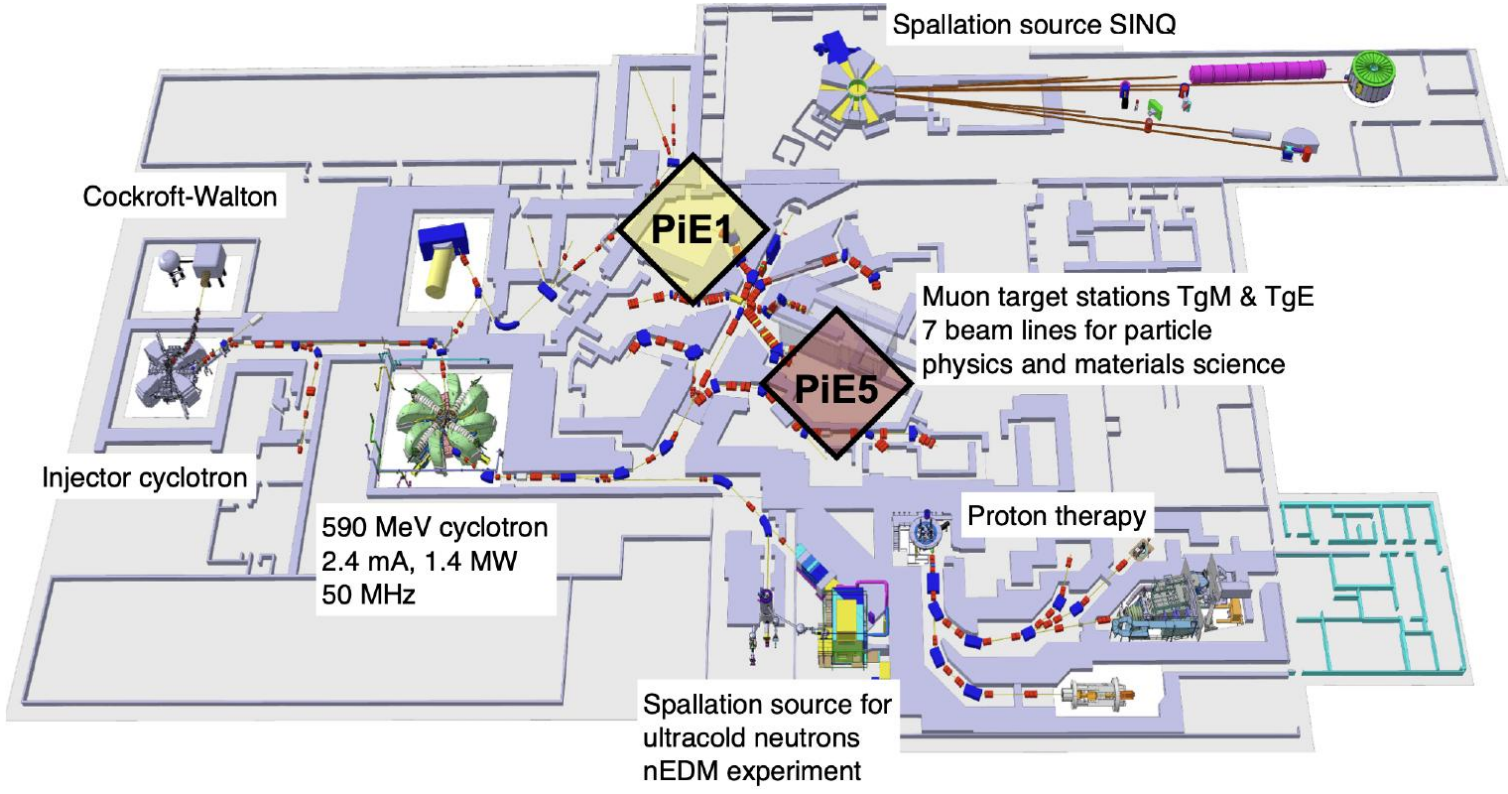

Principle

- Stop muon in 1mm H_2 gas at 22 K , 0.5 bar
- Wait until μp atoms de-excite and thermalize

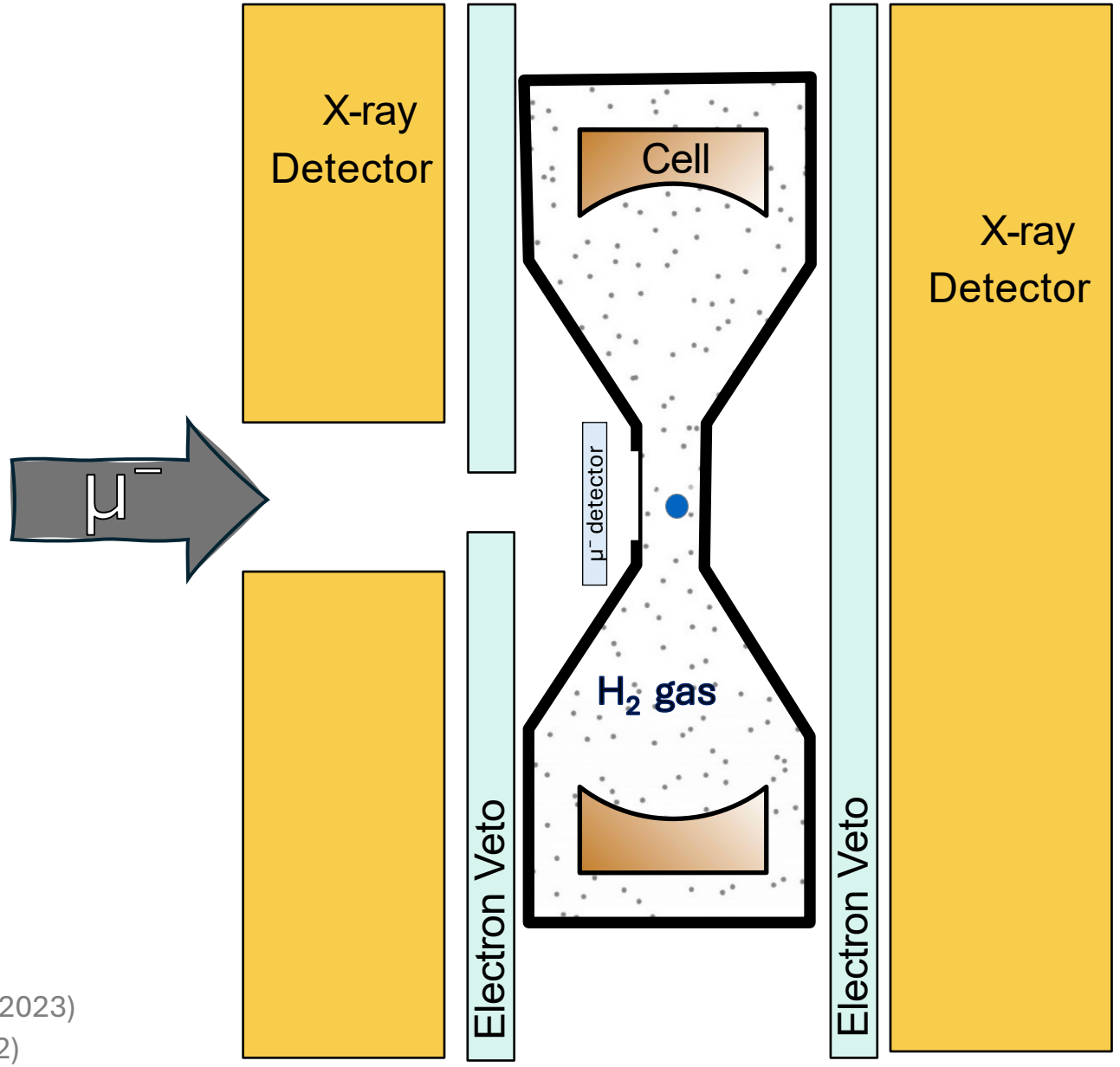

Nuber et al., SciPost Phys. Core 6, 057 (2023)
Amaro et al. SciPost Phys. 13, 020 (2022)

Principle

- Stop muon in 1mm H_2 gas at 22 K , 0.5 bar
- Wait until μp atoms de-excite and thermalize

- Laser pulse : μp(F=0) + γ → μp(F=1)
- De-excitation : μp(F=1) + H_2 → μp(F=0) + H_2 + E_{kin}

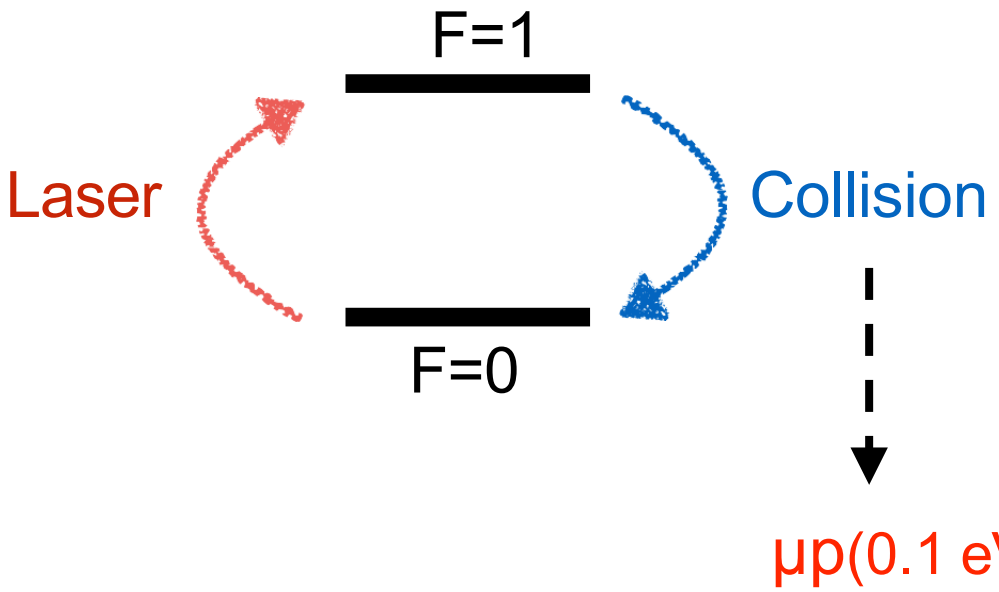

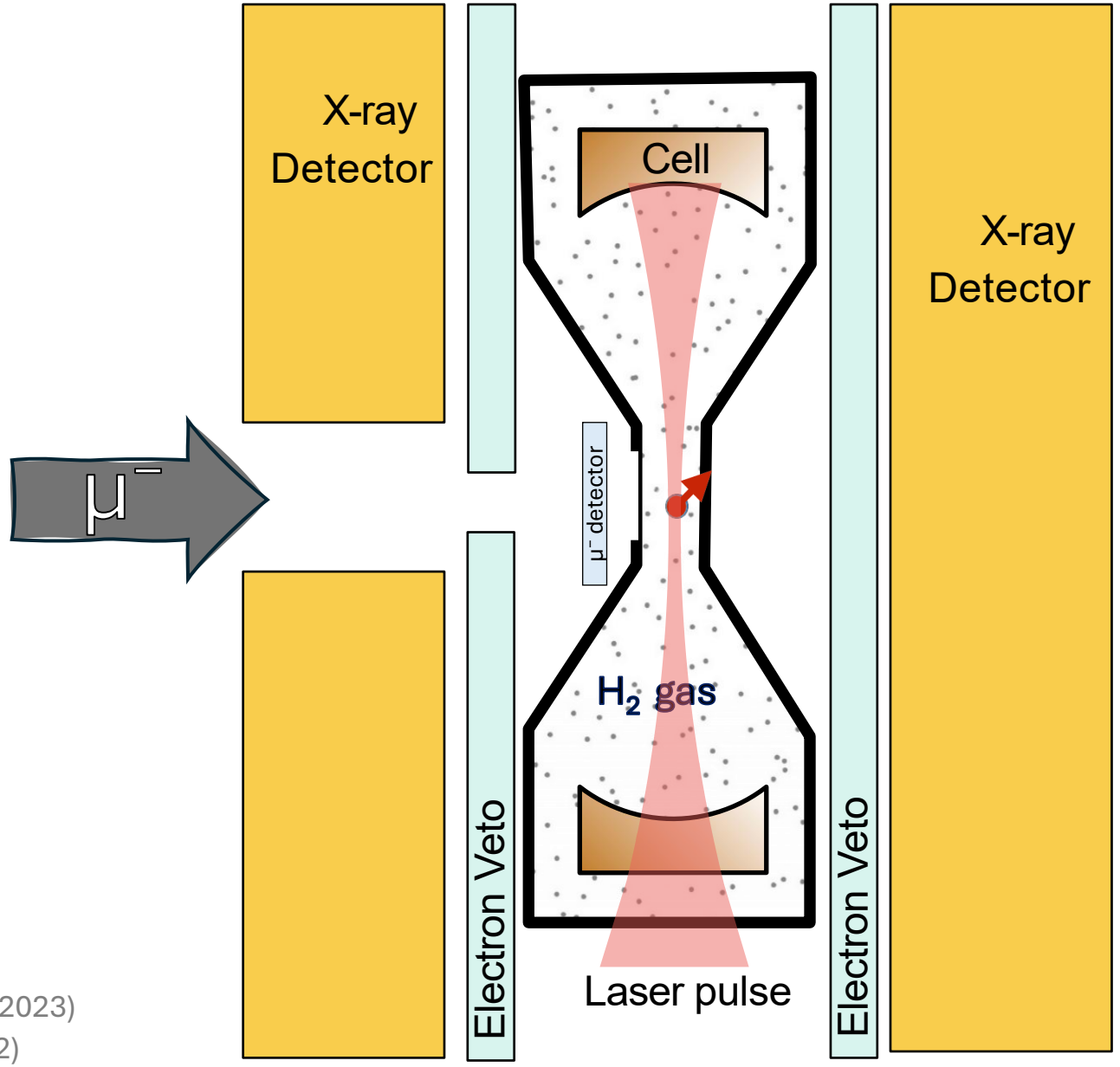

Nuber et al., SciPost Phys. Core 6, 057 (2023)
Amaro et al. SciPost Phys. 13, 020 (2022)

Principle

- Stop muon in 1mm H_2 gas at 22 K , 0.5 bar
- Wait until μp atoms de-excite and thermalize

- Laser pulse : μp(F=0) + γ → μp(F=1)
- De-excitation : μp(F=1) + H_2 → μp(F=0) + H_2 + E_{kin}

- μp diffuses to Au-coated target walls
- formed μAu* de-excites producing X-rays

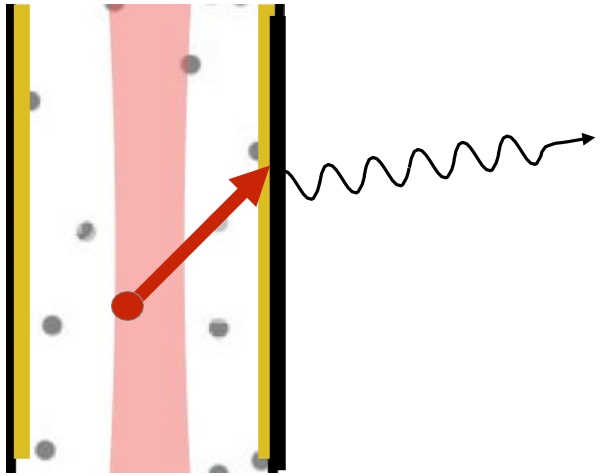

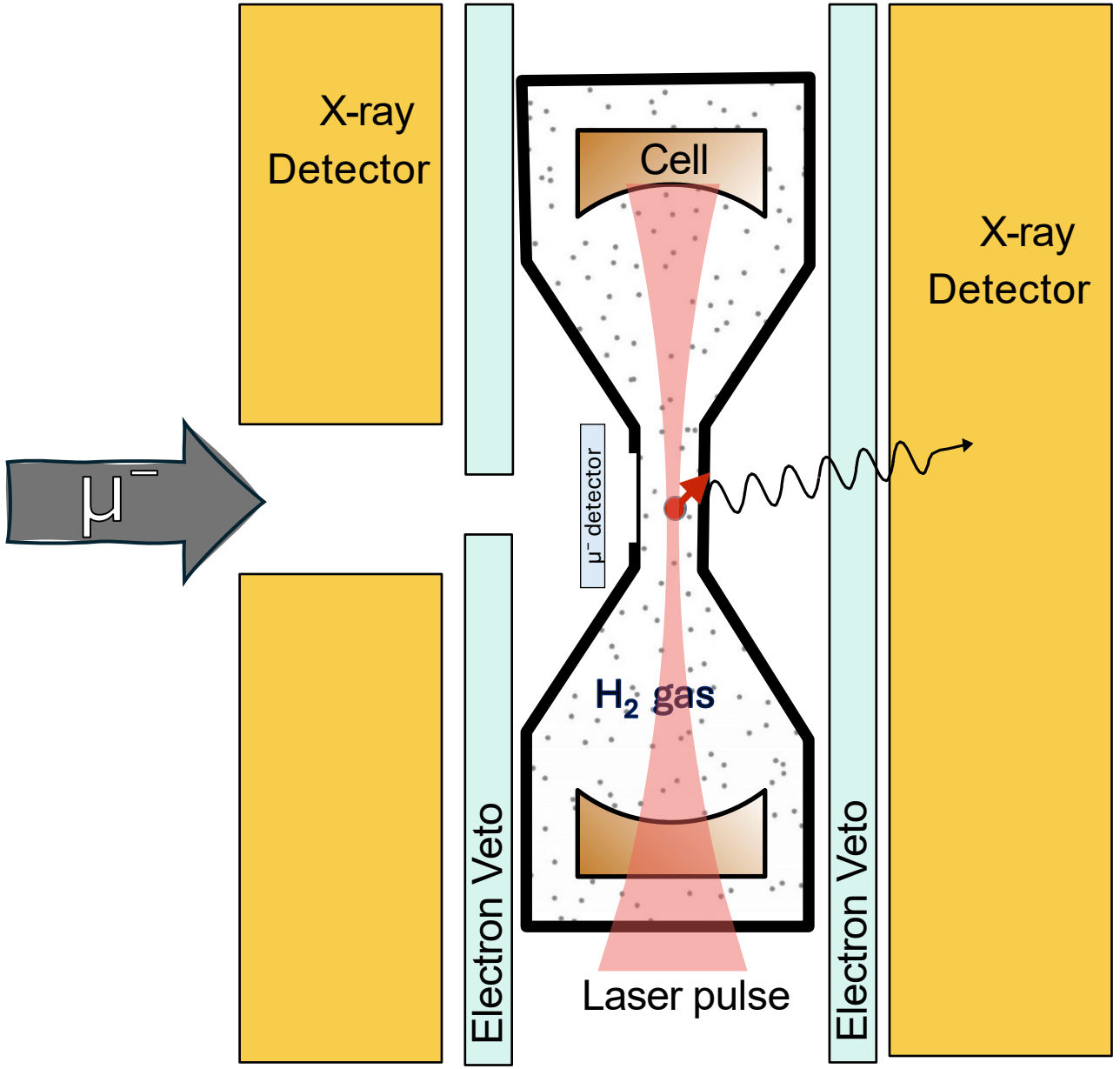

Principle

- Stop muon in 1mm H_2 gas at 22 K , 0.5 bar
- Wait until μp atoms de-excite and thermalize

- Laser pulse : μp(F=0) + γ → μp(F=1)
- De-excitation : μp(F=1) + H_2 → μp(F=0) + H_2 + E_{kin}

- μp diffuses to Au-coated target walls
- formed μAu* de-excites producing X-rays

- Plot number of μAu X-ray event vs laser frequency

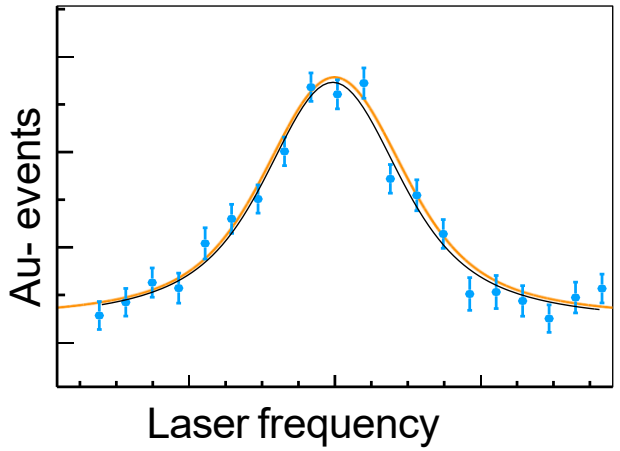

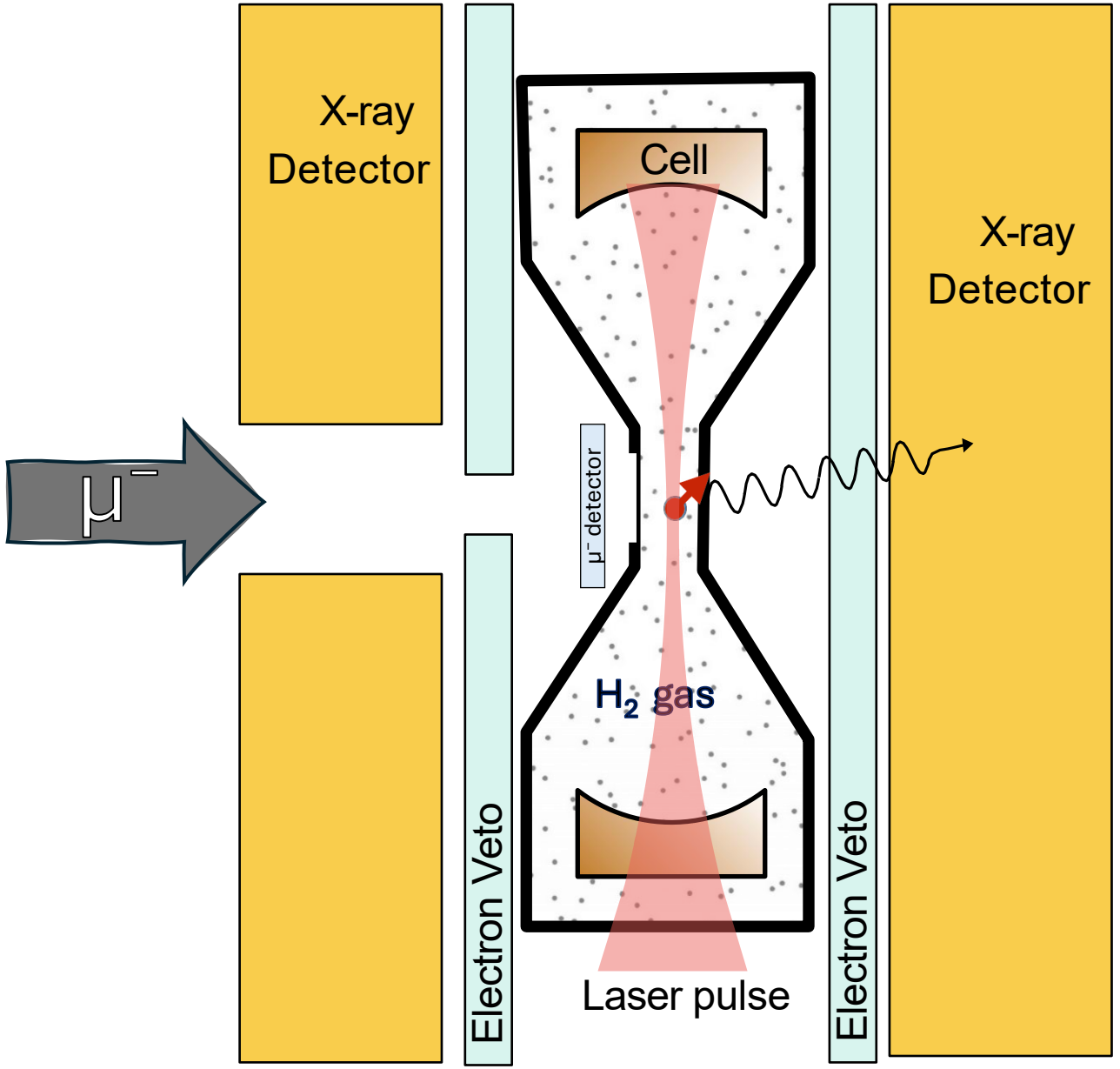

Laser excitation – Optical Bloch equation

Magnetic dipole (M1) transition

$$H_{\text{int}} = -\boldsymbol{\mu} \cdot \mathbf{B}(\mathbf{r})$$

$$\boldsymbol{\mu} = -g_e \mu_B \frac{\mathbf{S}}{\hbar} + g_p \mu_N \frac{\mathbf{I}}{\hbar}$$

muon proton

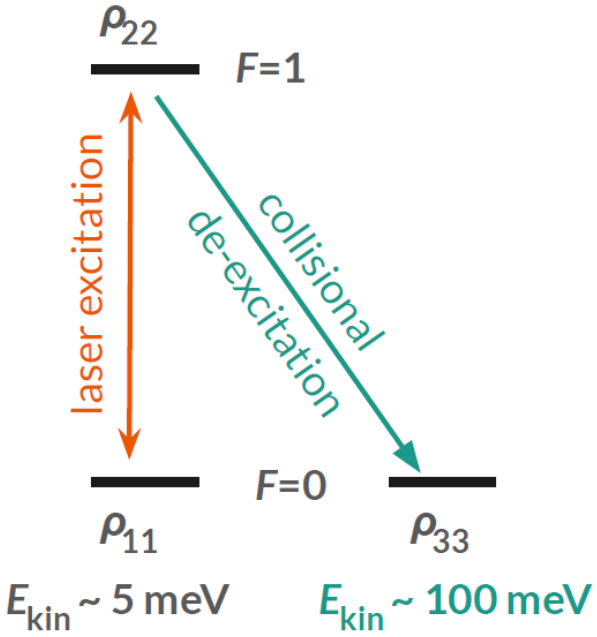

$$\begin{aligned}
\frac{d\rho_{11}}{dt}(t) &= -\mathrm{Im}\left(\Omega\rho_{12}e^{i\Delta t}\right) + \Gamma_{sp}\rho_{22}\,, \\
\frac{d\rho_{22}}{dt}(t) &= \mathrm{Im}\left(\Omega\rho_{12}e^{i\Delta t}\right) - (\Gamma_i + \Gamma_{sp})\rho_{22}\,, \\
\frac{d\rho_{12}}{dt}(t) &= \frac{i\Omega^*}{2}(\rho_{11} - \rho_{22})e^{-i\Delta t} - \frac{\Gamma_c}{2}\rho_{12}\,, \\
\frac{d\rho_{33}}{dt}(t) &= \Gamma_i\rho_{22}\,,
\end{aligned}$$

- ❑ Inelastic collisions
- ❑ Elastic collisions
- ❑ Laser bandwidth
- ❑ Doppler broadening

Amaro et al. SciPost Phys. 13, 020 (2022)

Laser excitation – Lineshape

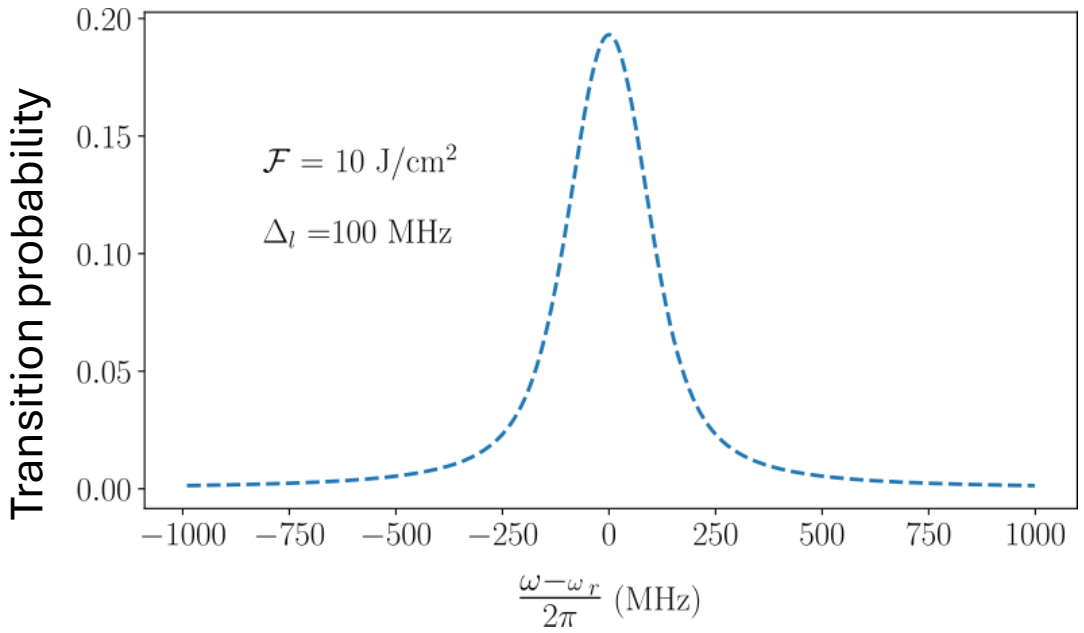

Amaro et al. SciPost Phys. 13, 020 (2022)

Laser excitation – Lineshape

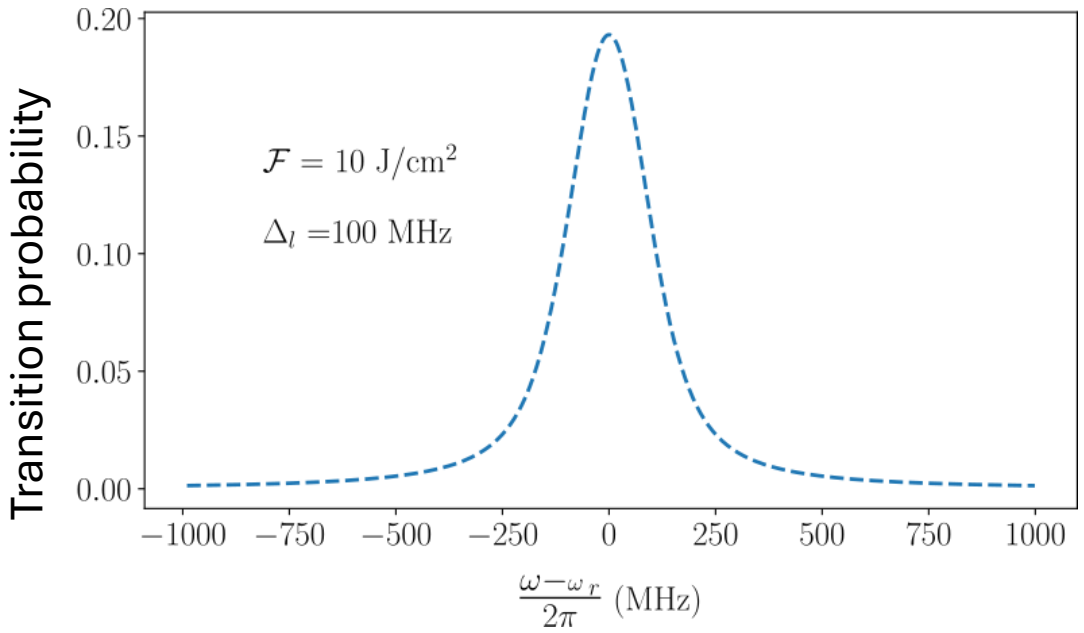

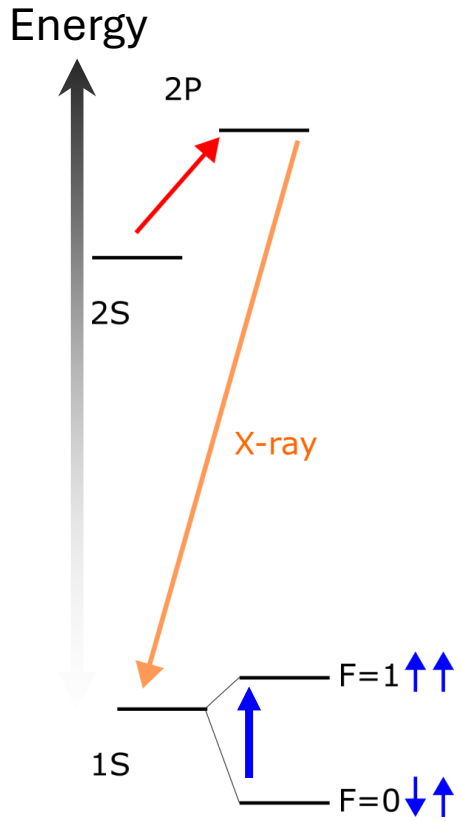

Transition	Linewidth	Saturation fluence	Wavelength	Signal:BG	Signal
2S-2P	20 GHz	0.016 J/cm^2	6.0μm	6:1	2P-1S in μH
HFS	200 MHz	44 J/cm^2	6.8μm	1:10	X-ray from μAu

Amaro et al. SciPost Phys. 13, 020 (2022)

Laser system

- ~2 mJ of 6.8 μm, τ=50 ns
- < 100 MHz bandwidth
- >40 GHz tunability
- 200 1/s rep. rate
- TEM_{00} beam M^2 ~1
- Stochastic trigger, latency <1 μs

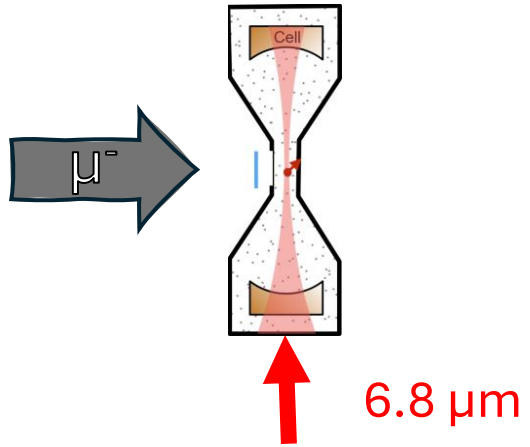

Laser system

- ~2 mJ of 6.8 µm, τ=50 ns
- < 100 MHz bandwidth
- >40 GHz tunability
- 200 1/s rep. rate
- TEM_{00} beam M^2 ~1
- Stochastic trigger, latency <1 µs

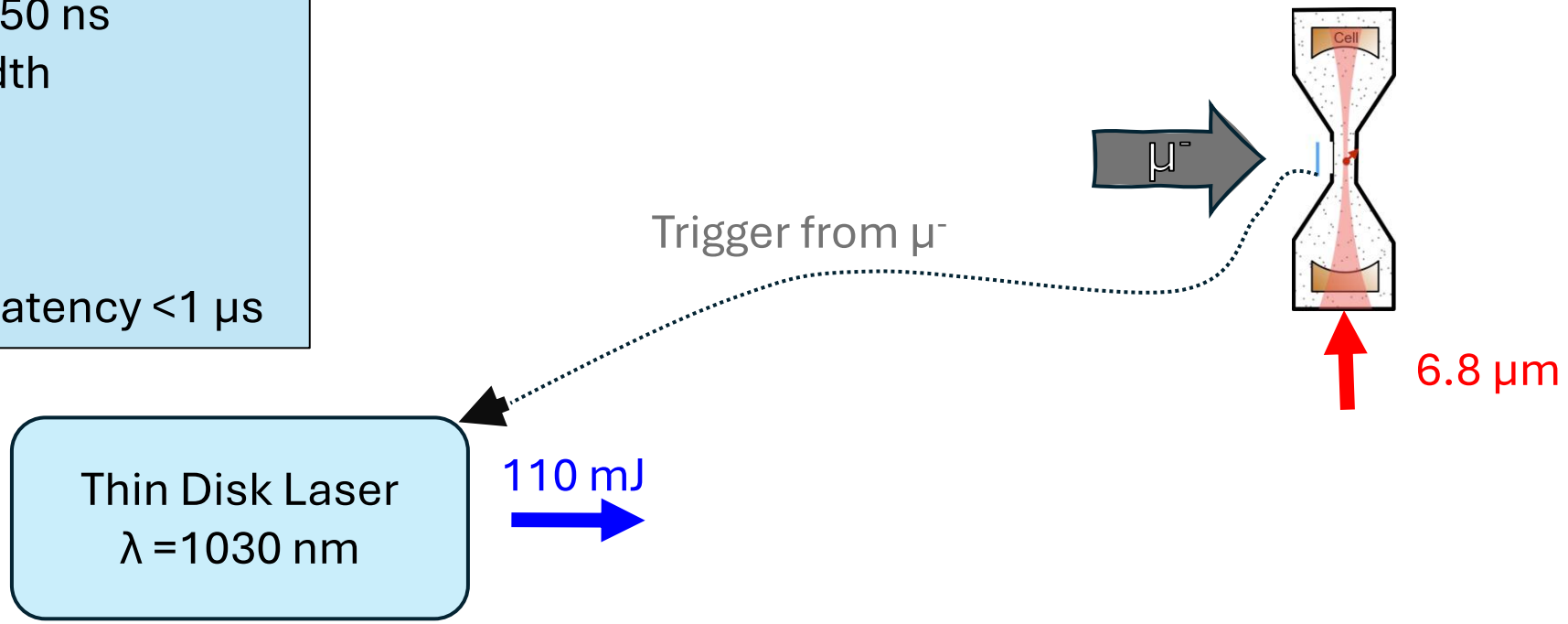

Laser system

- ~2 mJ of 6.8 µm, τ=50 ns
- < 100 MHz bandwidth
- >40 GHz tunability
- 200 1/s rep. rate
- TEM_{00} beam M^2 ~1
- Stochastic trigger, latency <1 µs

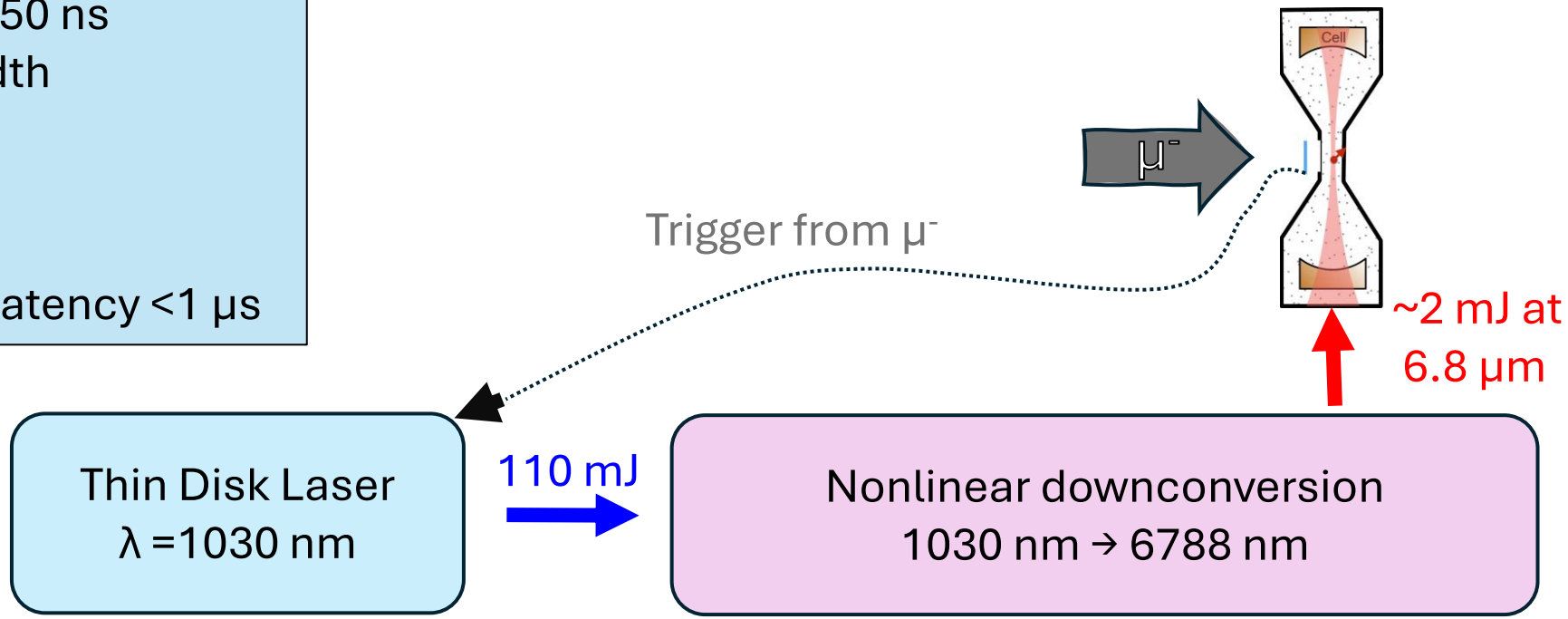

Laser system

- ~2 mJ of 6.8 μm, τ=50 ns
- < 100 MHz bandwidth
- >40 GHz tunability
- 200 1/s rep. rate
- TEM_{00} beam M^2 ~1
- Stochastic trigger, latency <1 μs

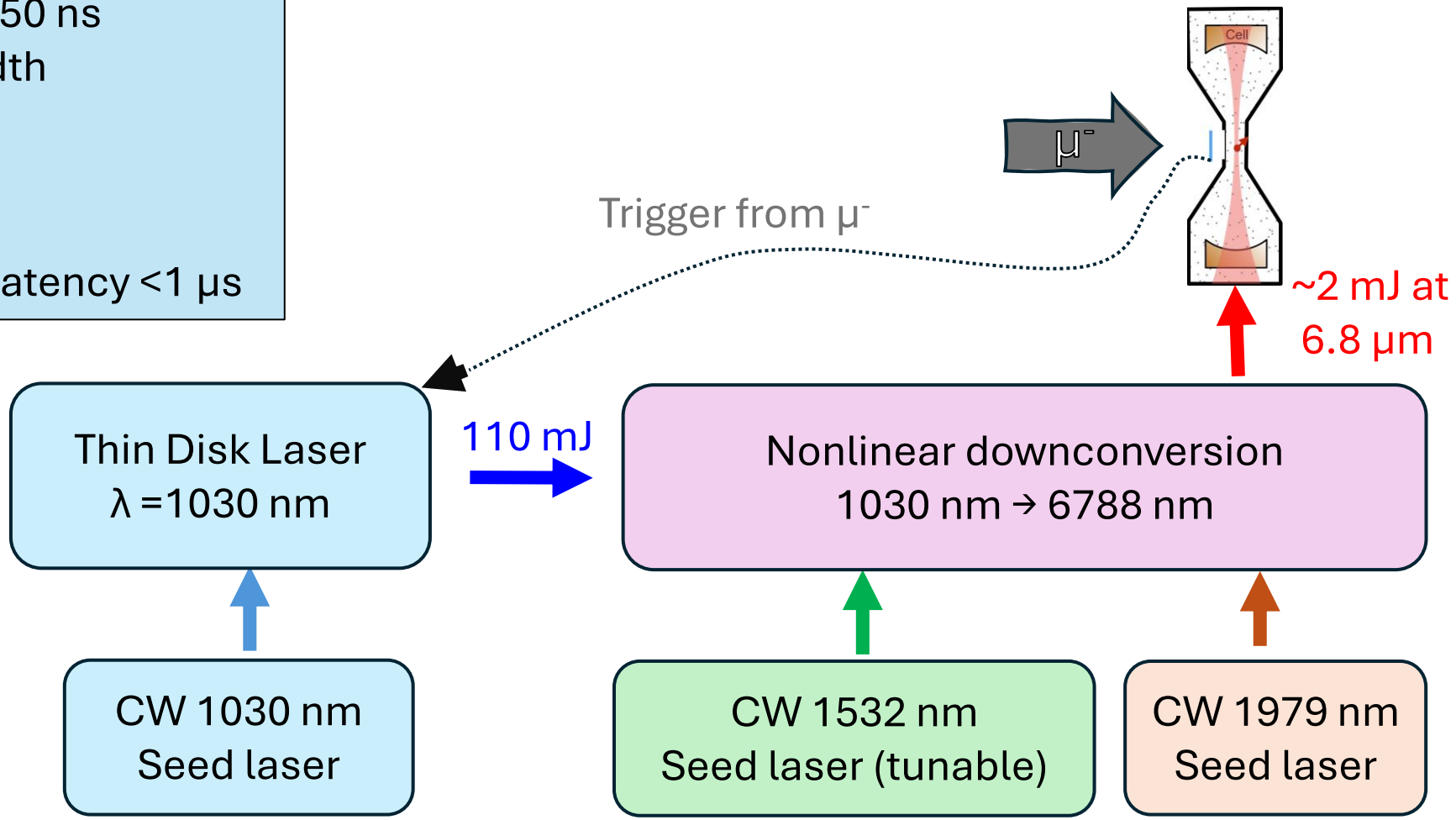

Laser system in reality

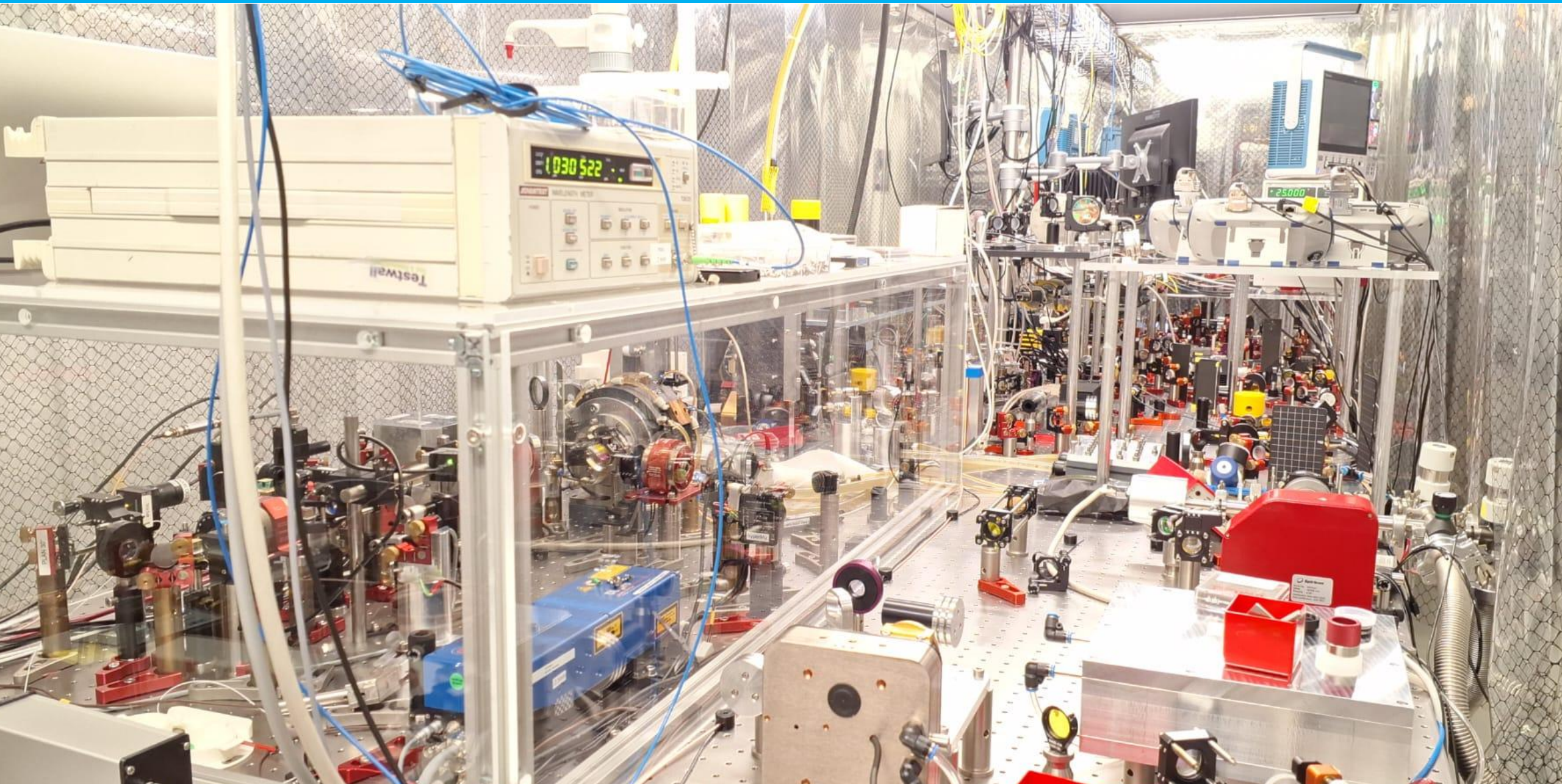

Laser system

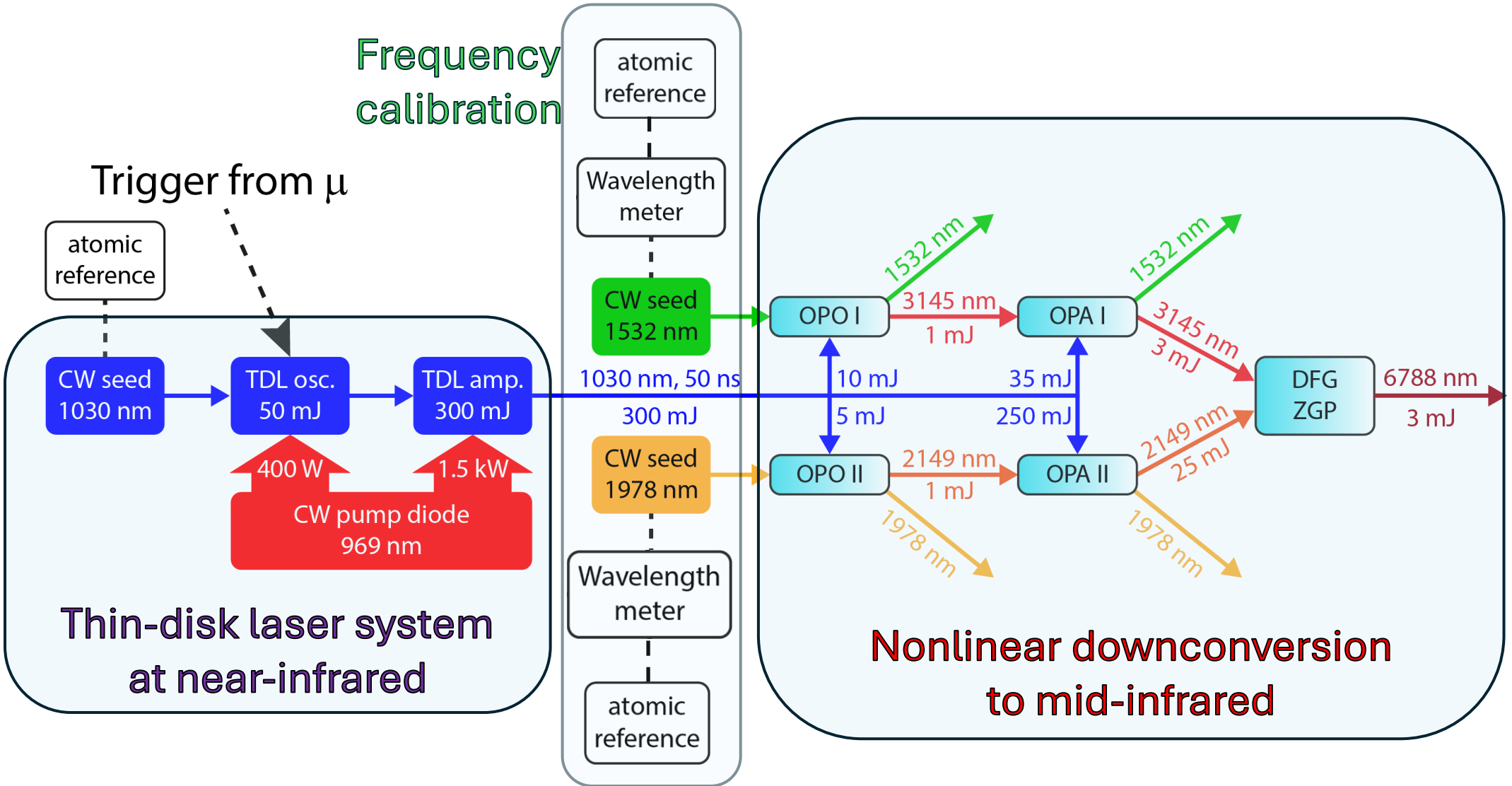

Laser system

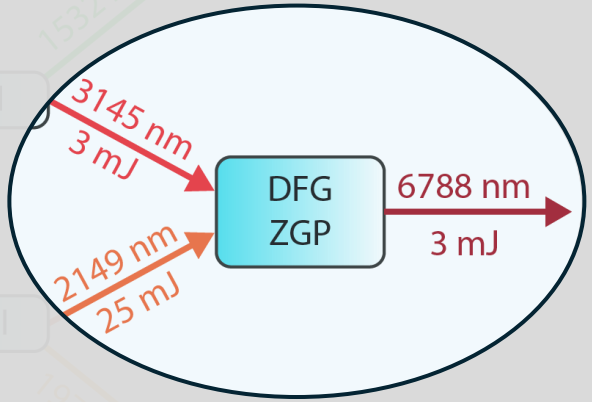

Laser system is ready

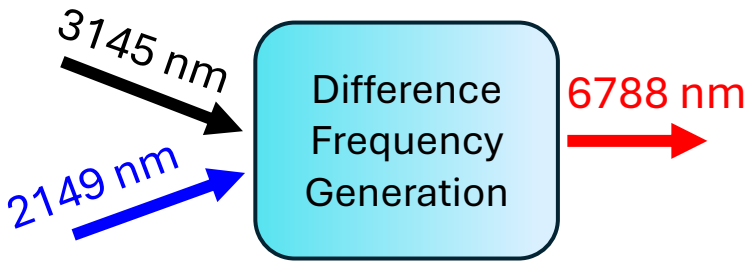

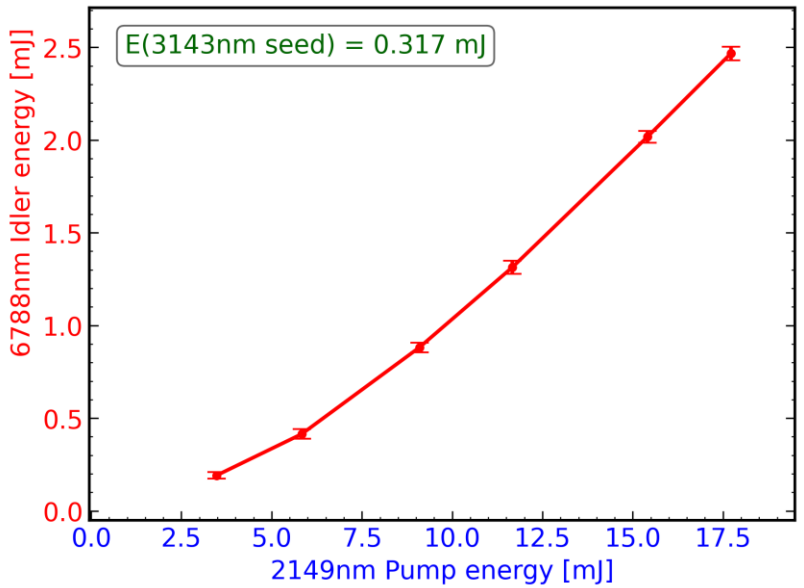

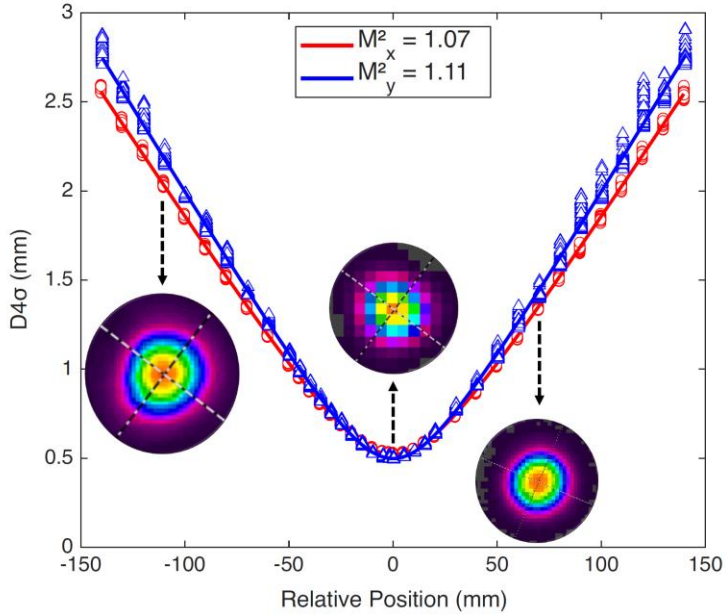

- ☑ ~2.4 mJ at 6788 nm
- ☑ >200 /s rep. rate
- ☑ M^2_{avg} ~ 1.09
- ☑ Frequency tunable

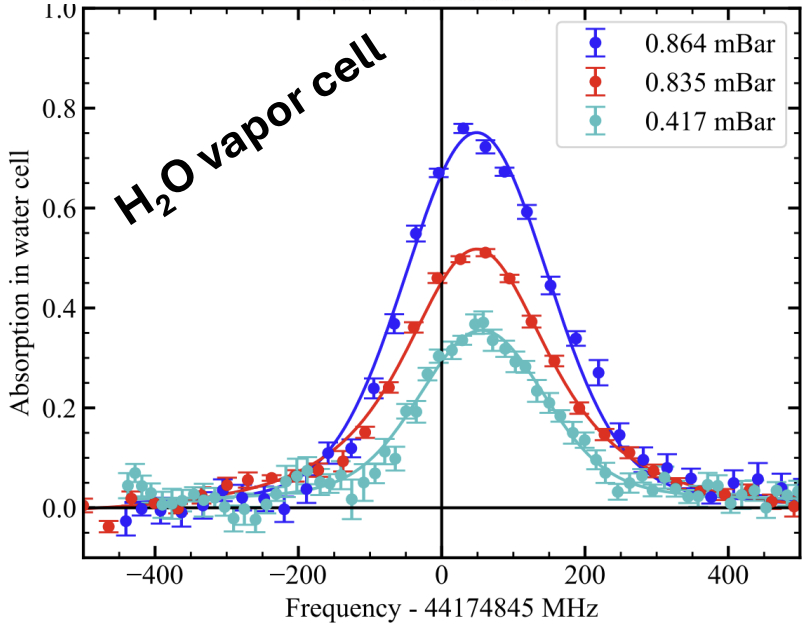

Multipass enhancement cell

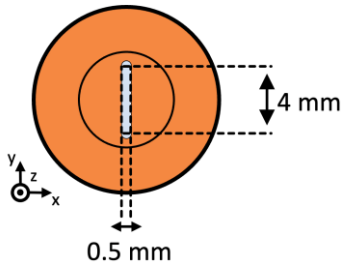

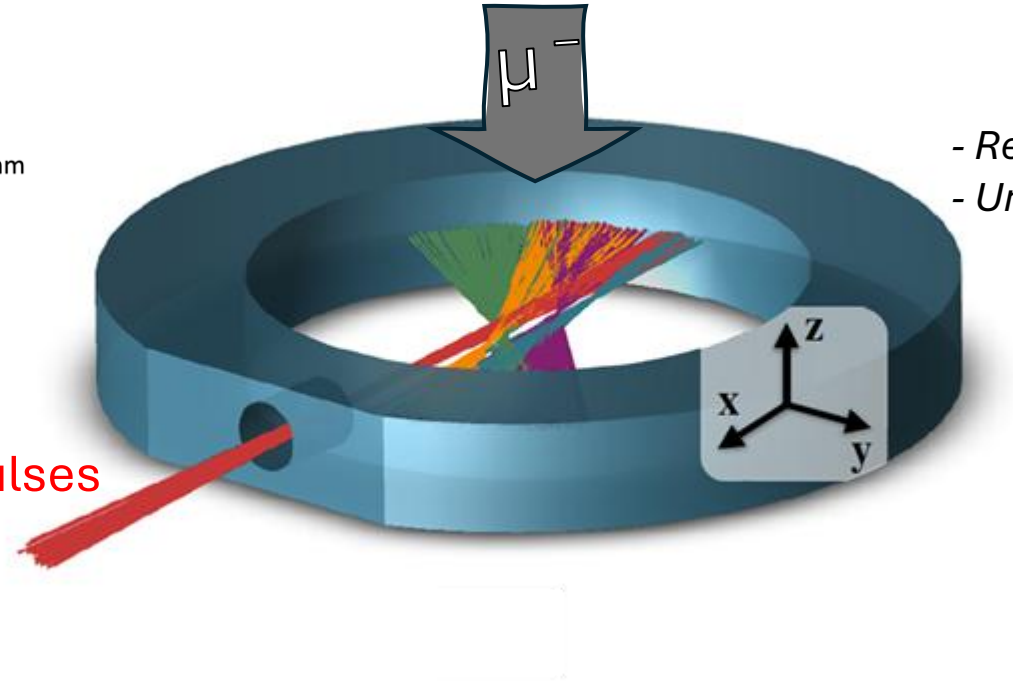

- *Resonant in z-axis*
- *Unstable in xy-plane*

- ❖ Tight alignment constraints
- ❖ High reflectivity
- ❖ Cryogenic compatible
- ❖ High fluence in muon stopping volume

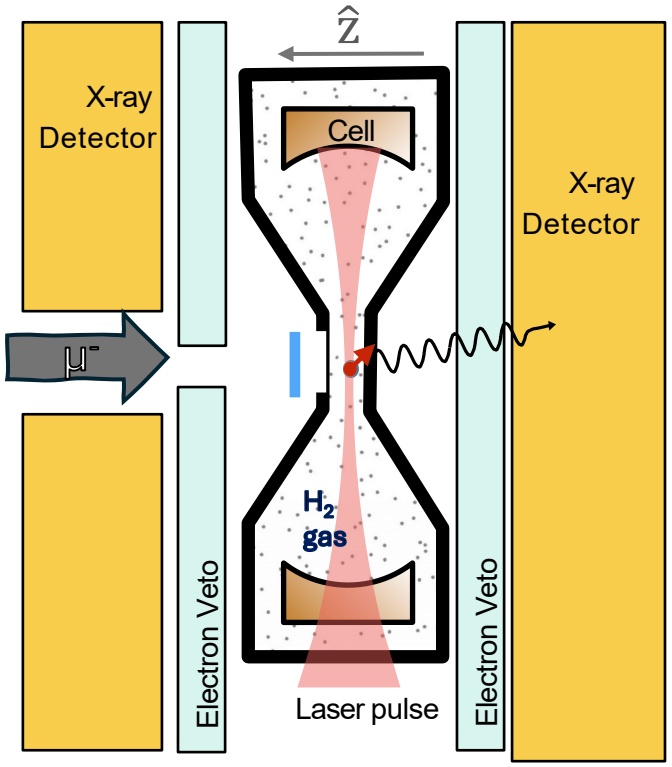

Multipass enhancement cell

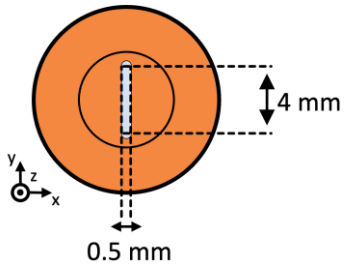

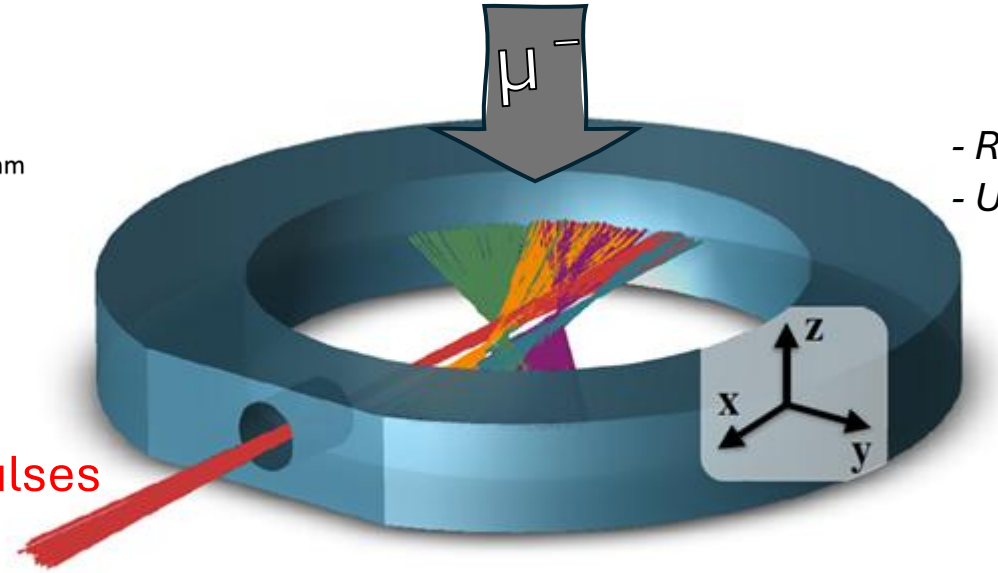

- *Resonant in z-axis*
- *Unstable in xy-plane*

- ❖ Tight alignment constraints
- ❖ High reflectivity
- ❖ Cryogenic compatible
- ❖ High fluence in muon stopping volume

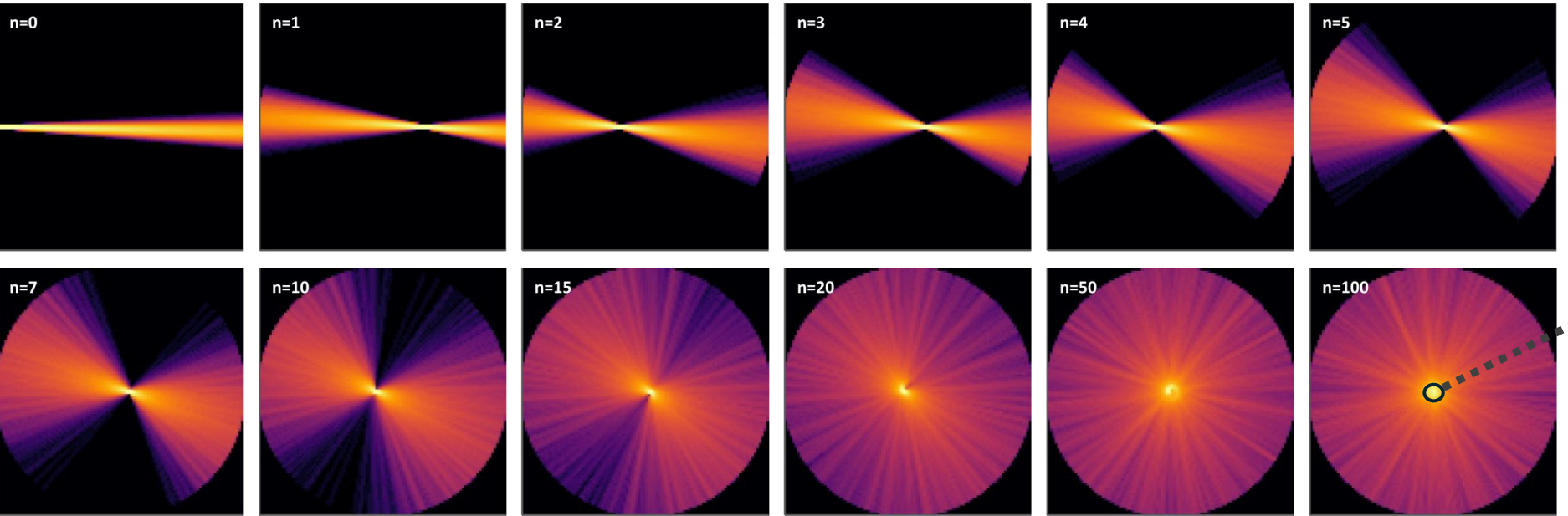

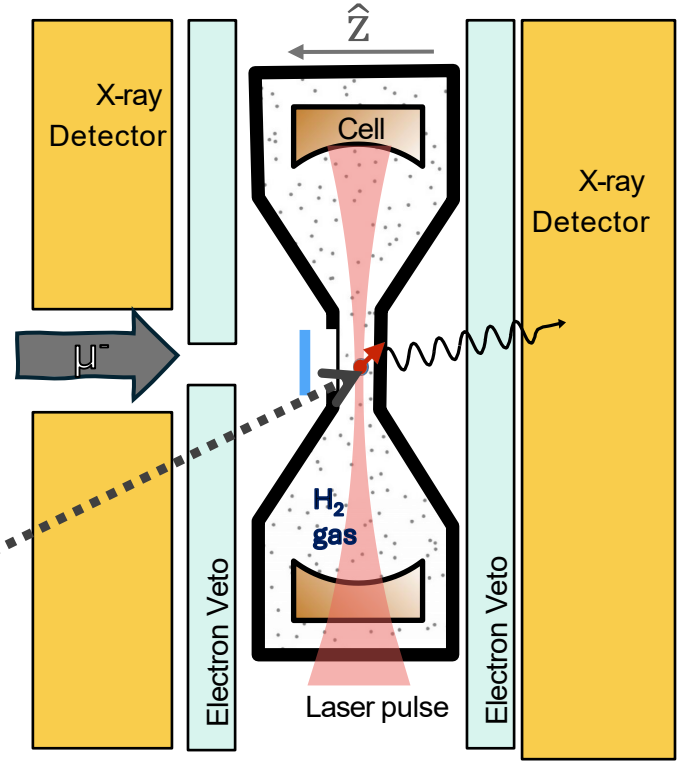

Multipass enhancement cell

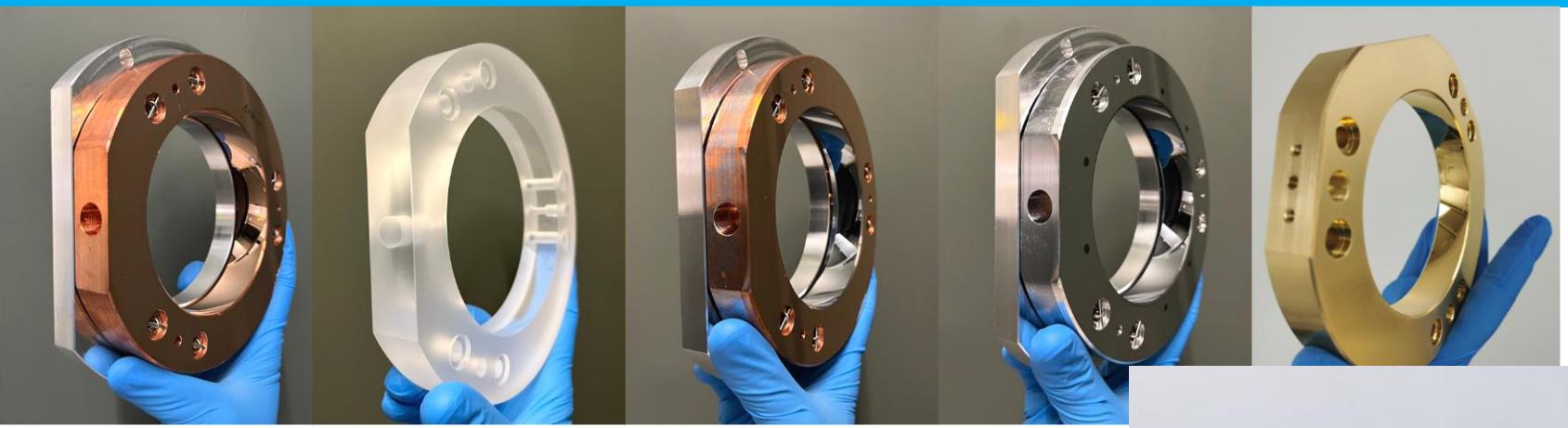

- Tested multiple coatings
- Measured reflectivity of 99.5% at 6.8 μm

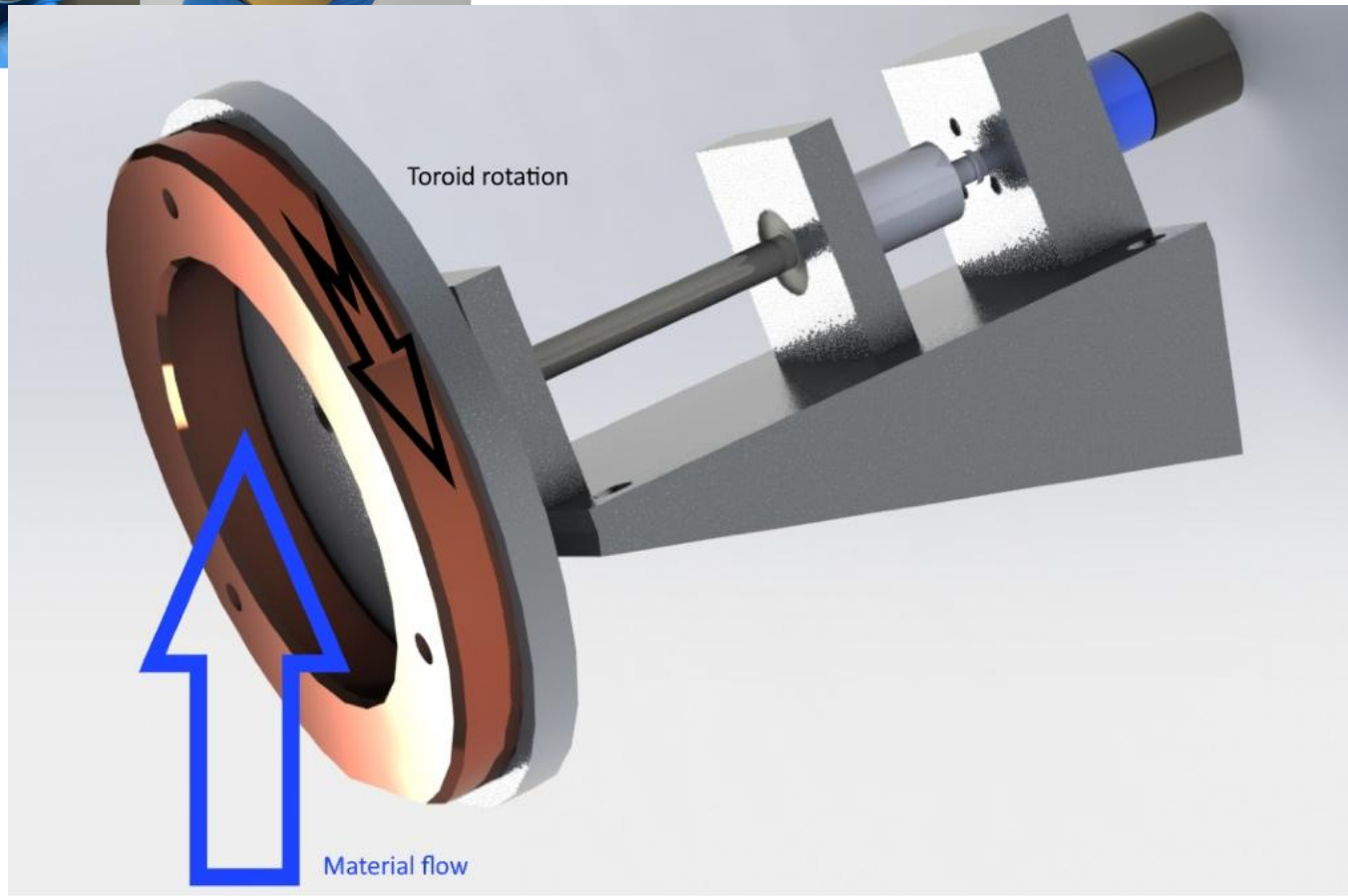

Multipass enhancement cell

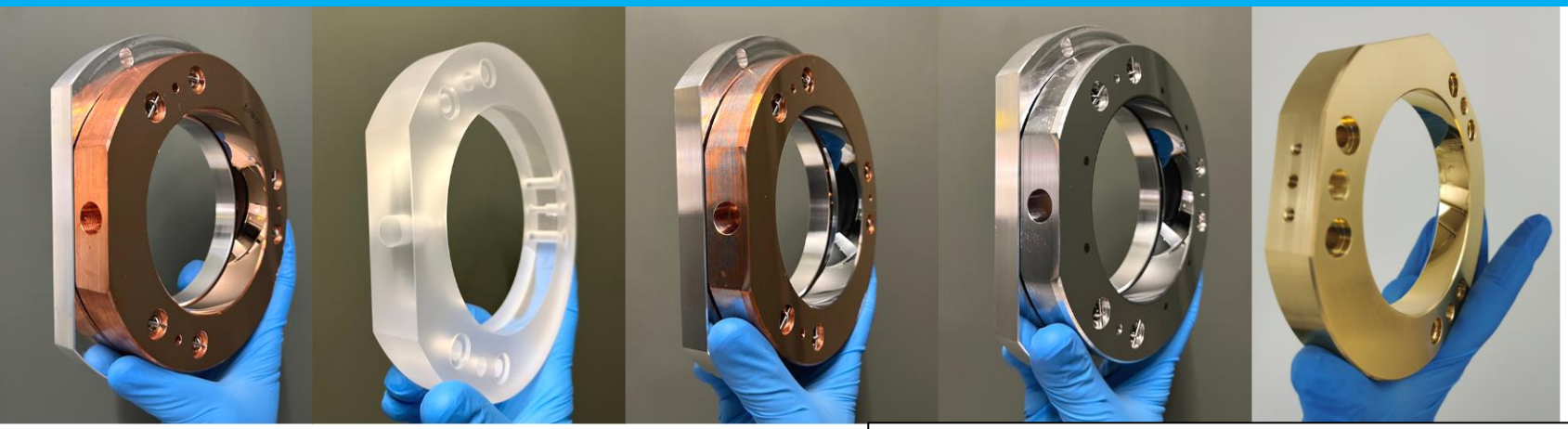

- Tested multiple coatings
- Measured reflectivity of 99.5% at 6.8 μm
- Test at 20 K

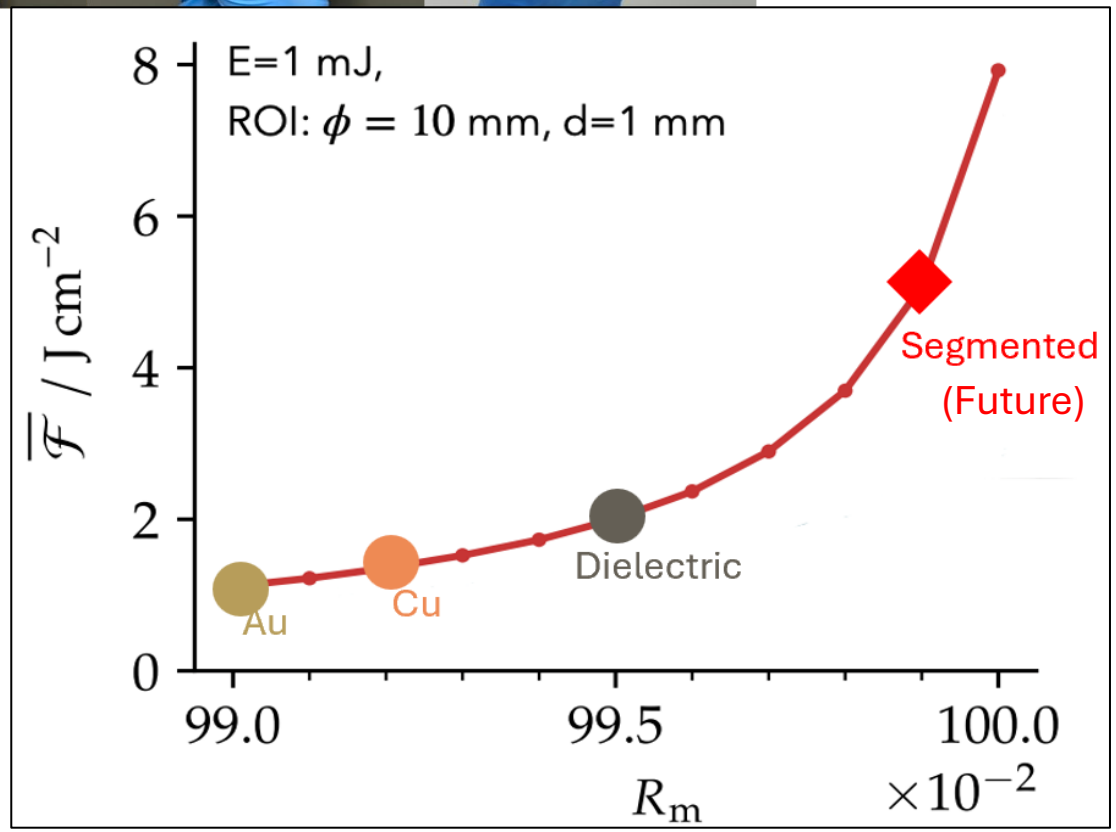

Multipass enhancement cell

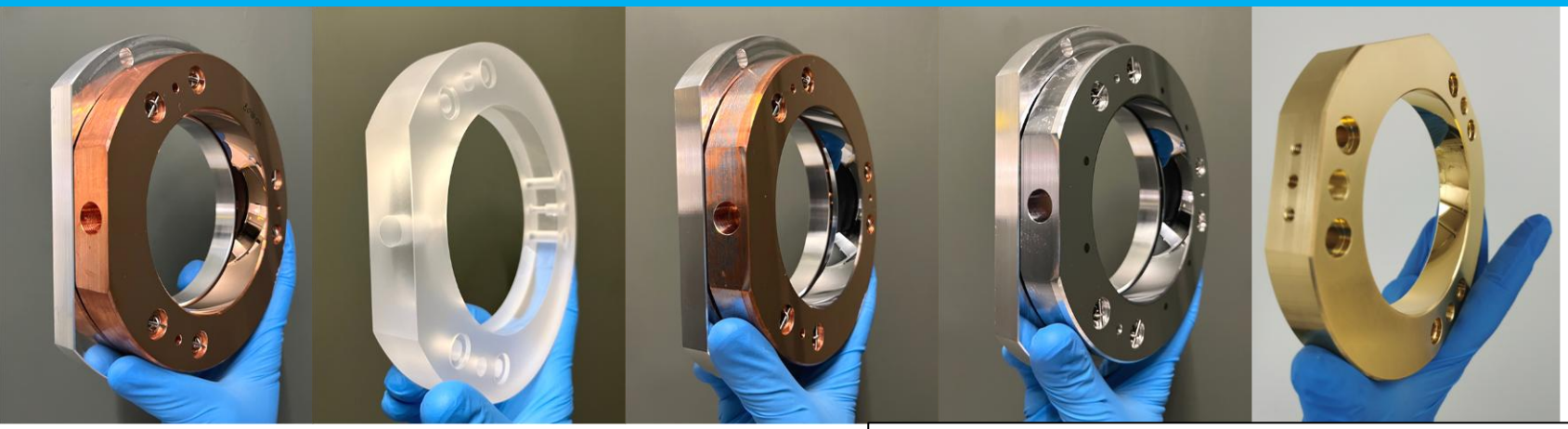

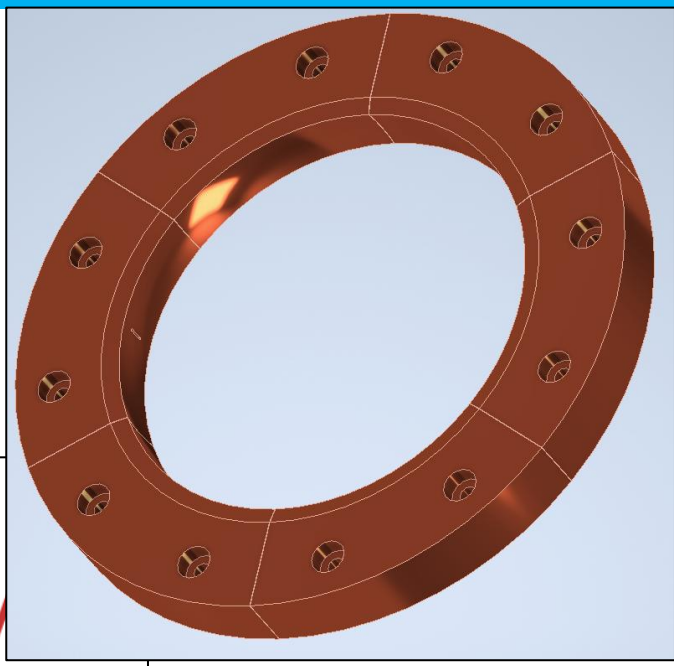

- Tested multiple coatings
- Measured reflectivity of 99.5% at 6.8 μm
- Test at 20 K
- Developing a Segmented cell (expected effective R ~ 99.9%)

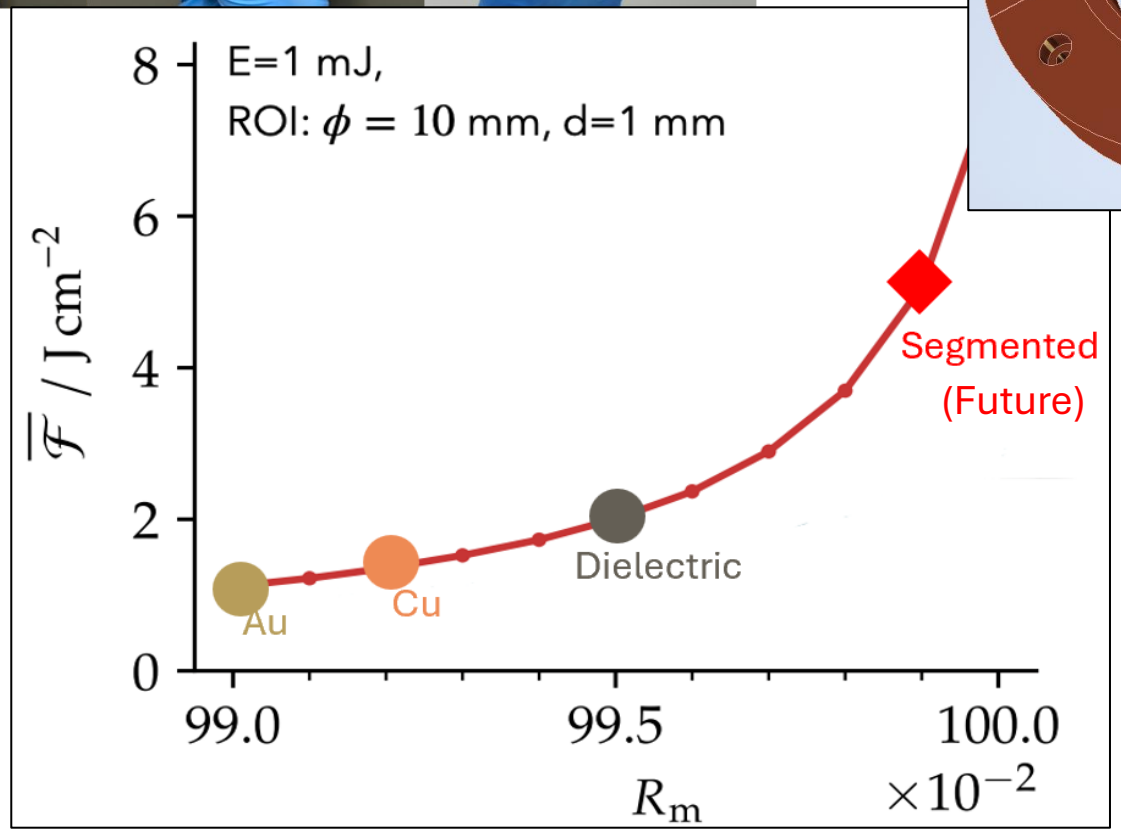

Signal and BG : Muon diffusion

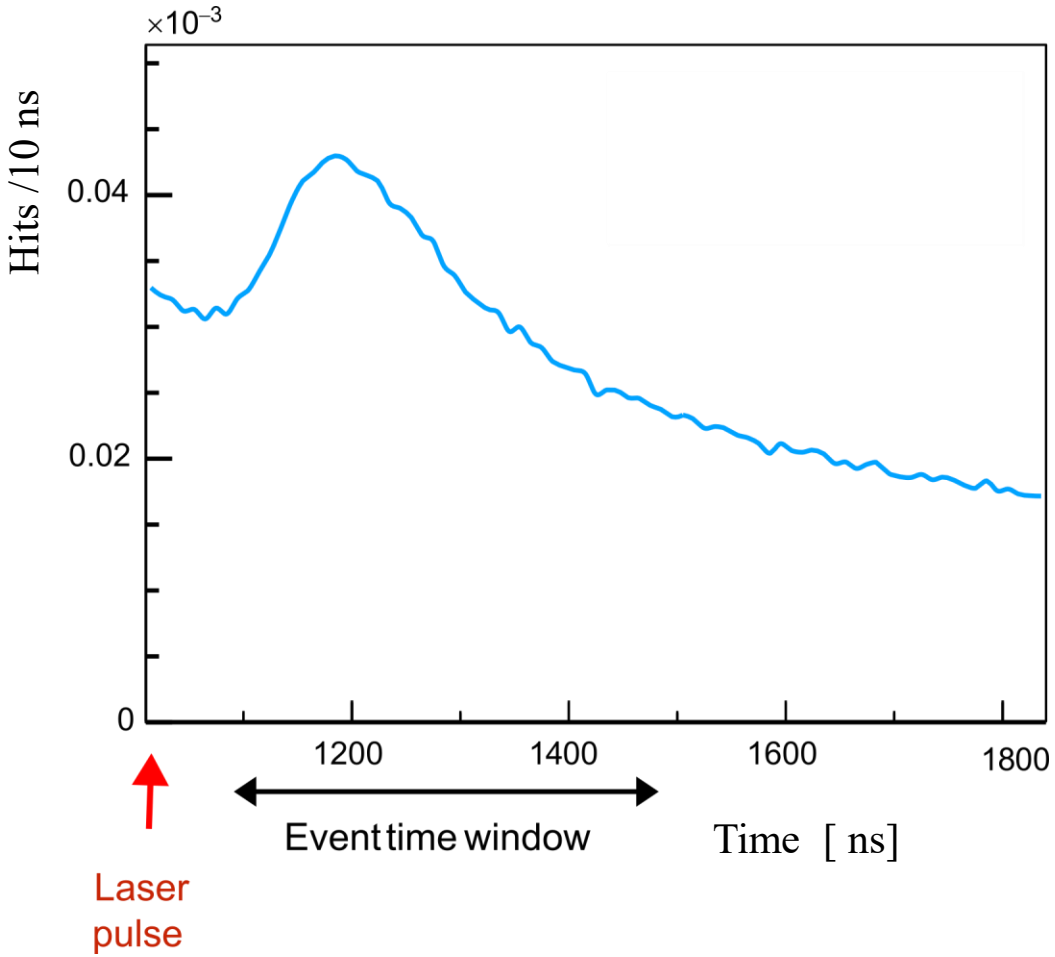

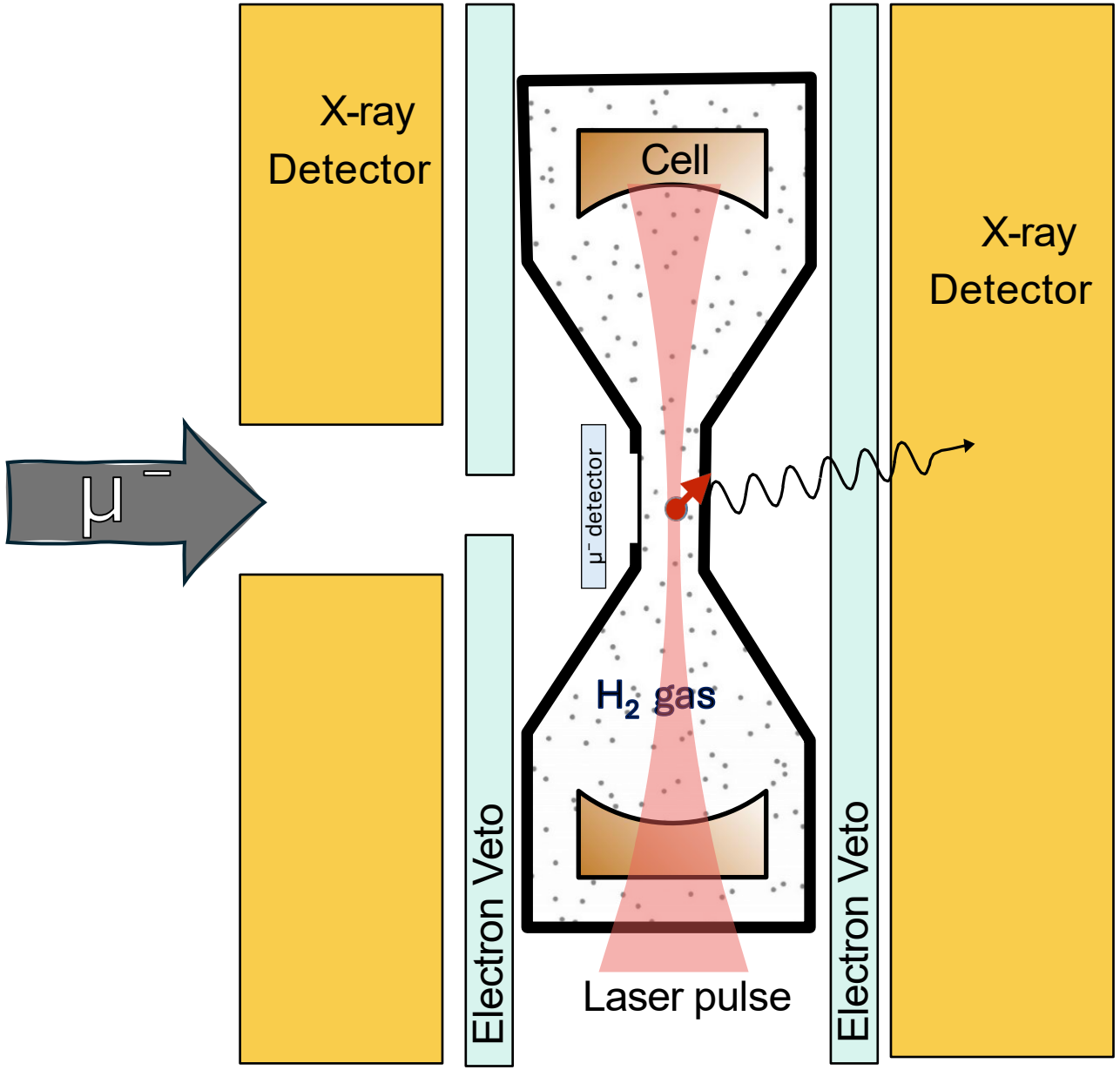

Nuber et al., SciPost Phys. Core 6, 057 (2023)

Signal and BG : Muon diffusion

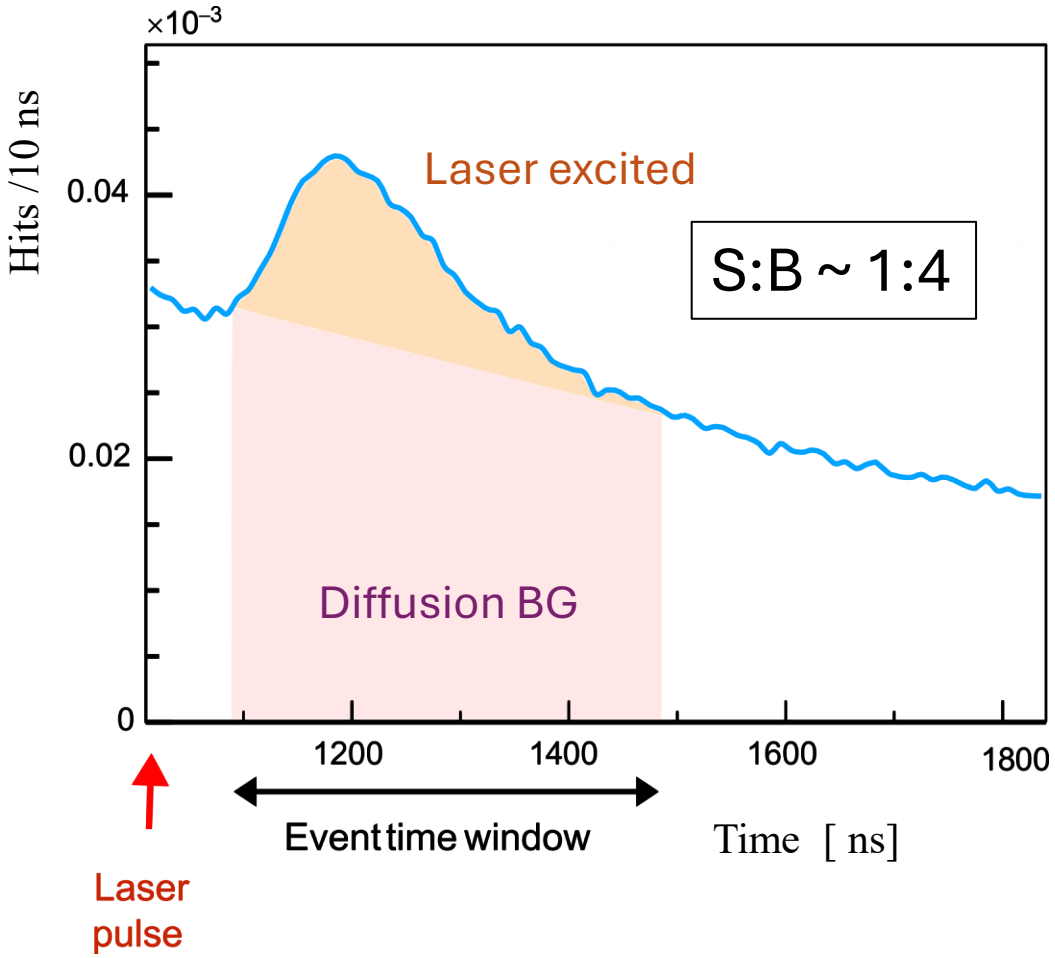

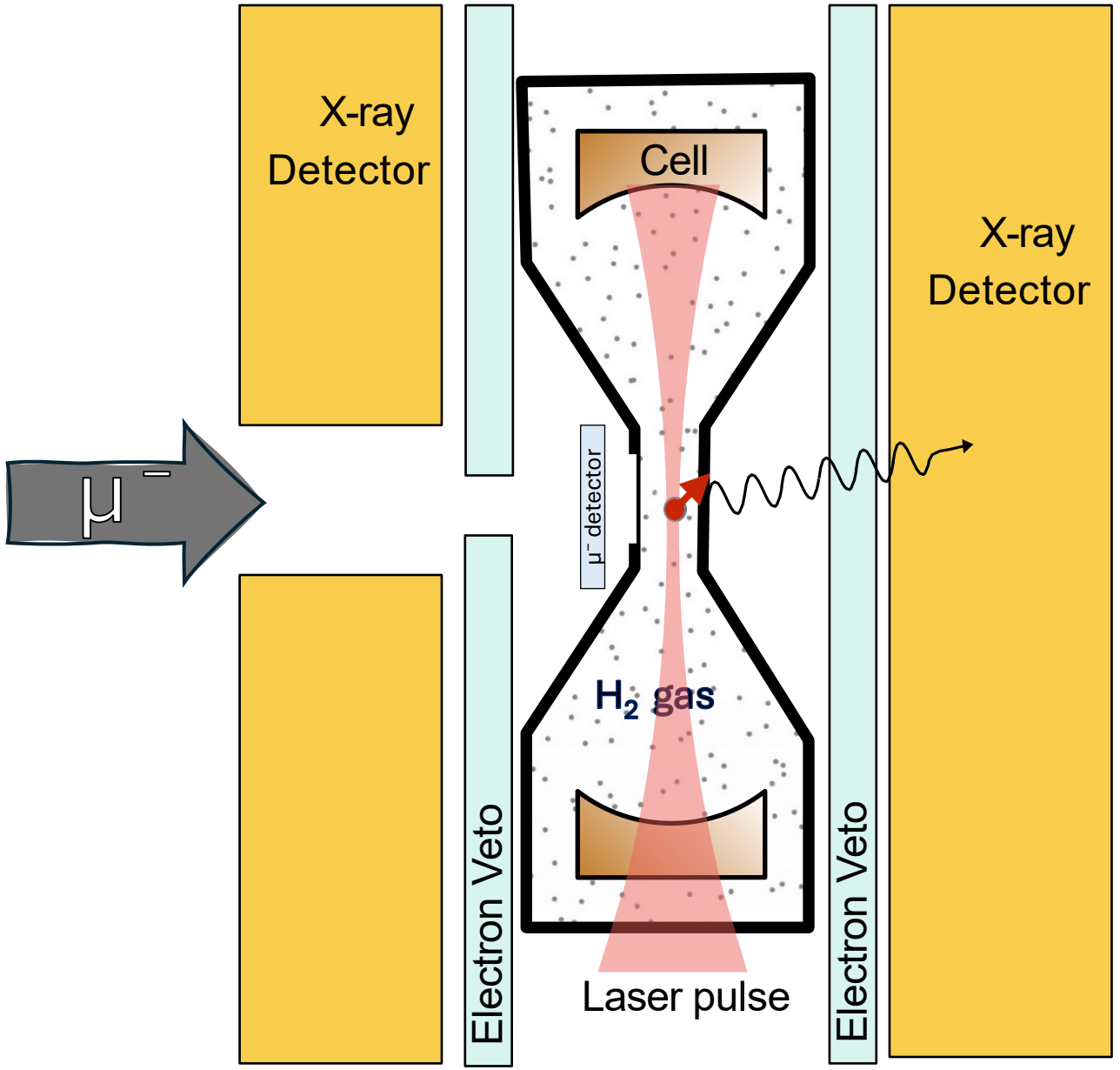

Nuber et al., SciPost Phys. Core 6, 057 (2023)

Signal and BG : Simulated resonance

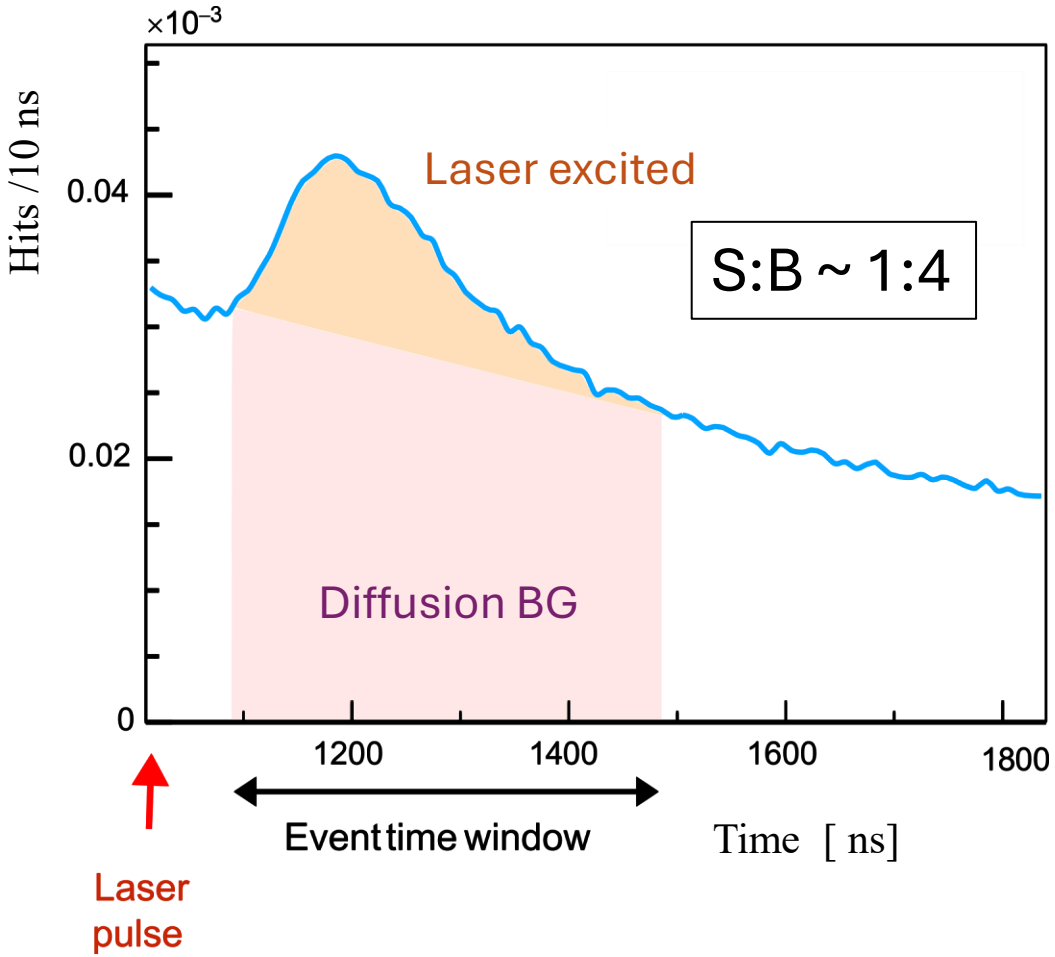

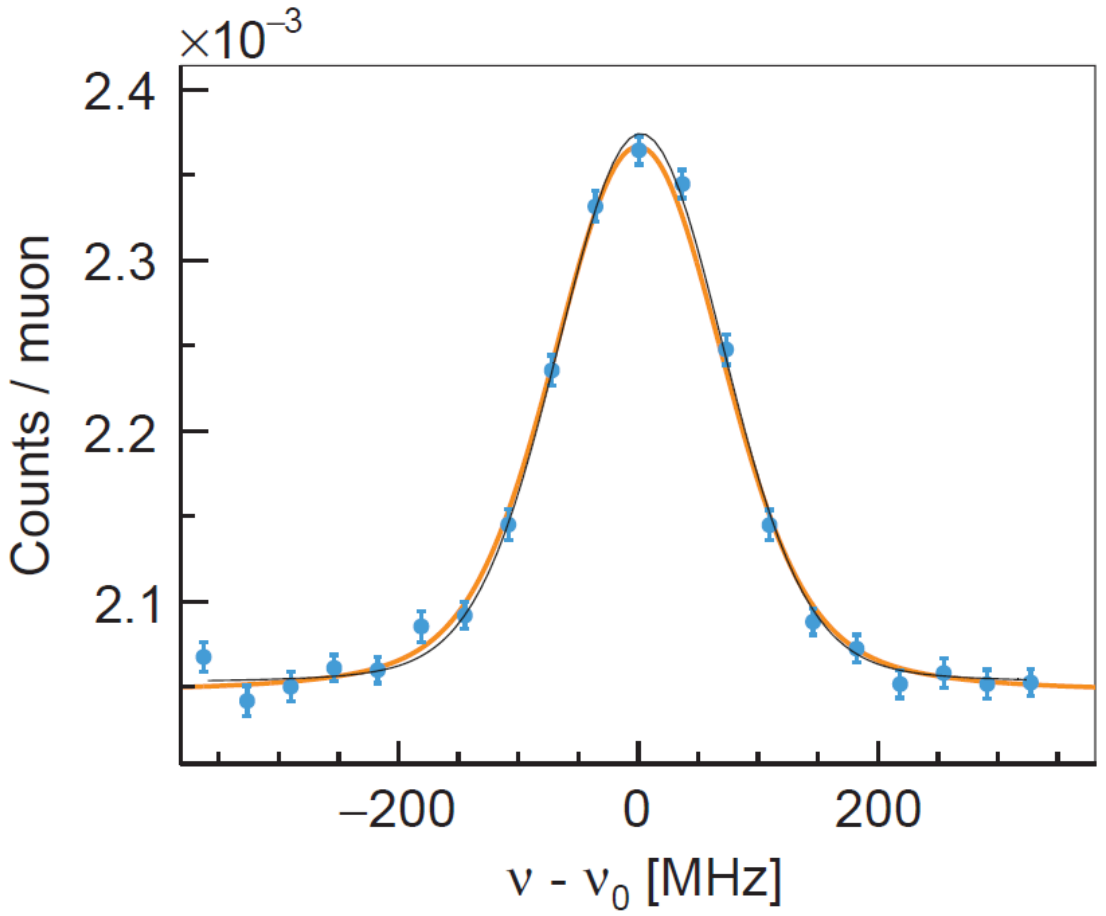

Nuber et al., SciPost Phys. Core 6, 057 (2023)

Signal and BG : Simulated resonance

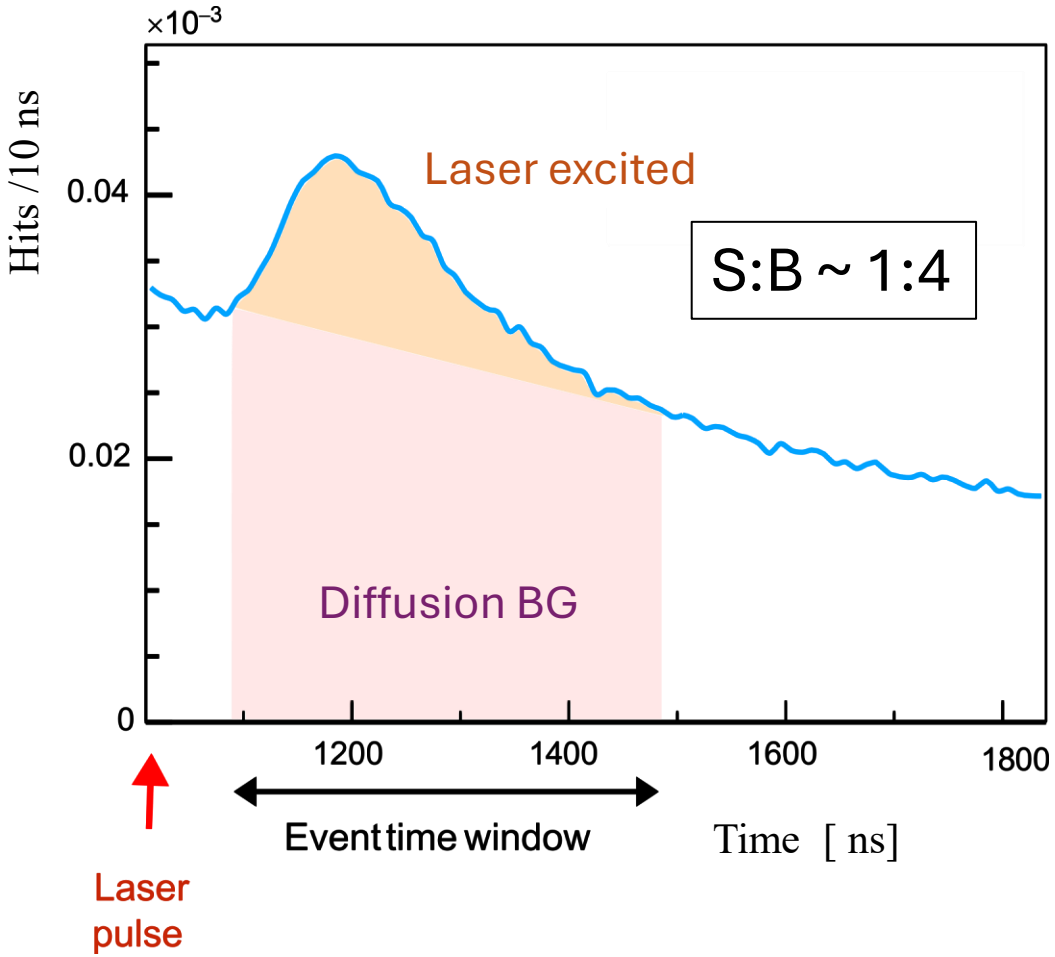

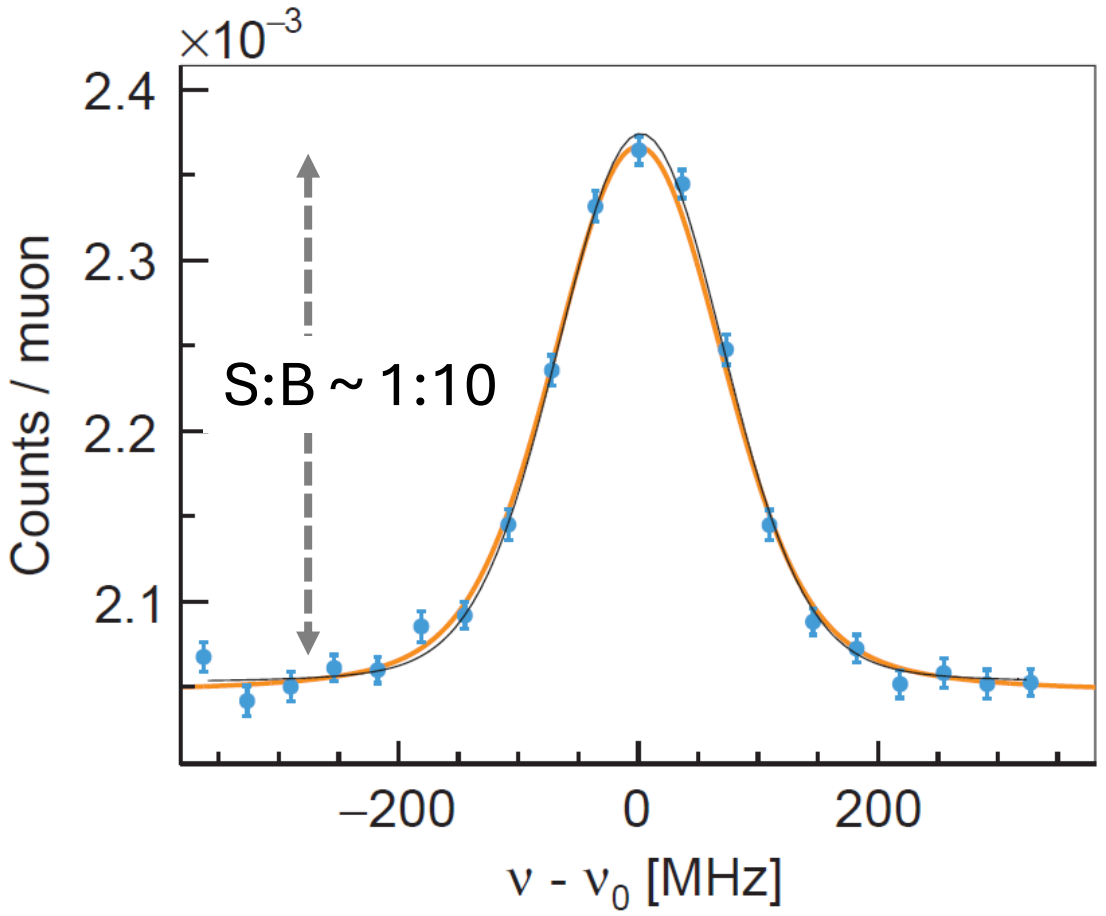

Nuber et al., SciPost Phys. Core 6, 057 (2023)

Signal and BG : Total background

$$\mu^- \xrightarrow[2.2\,\mu s]{} e^- + \bar{\nu}_e + \nu_\mu$$

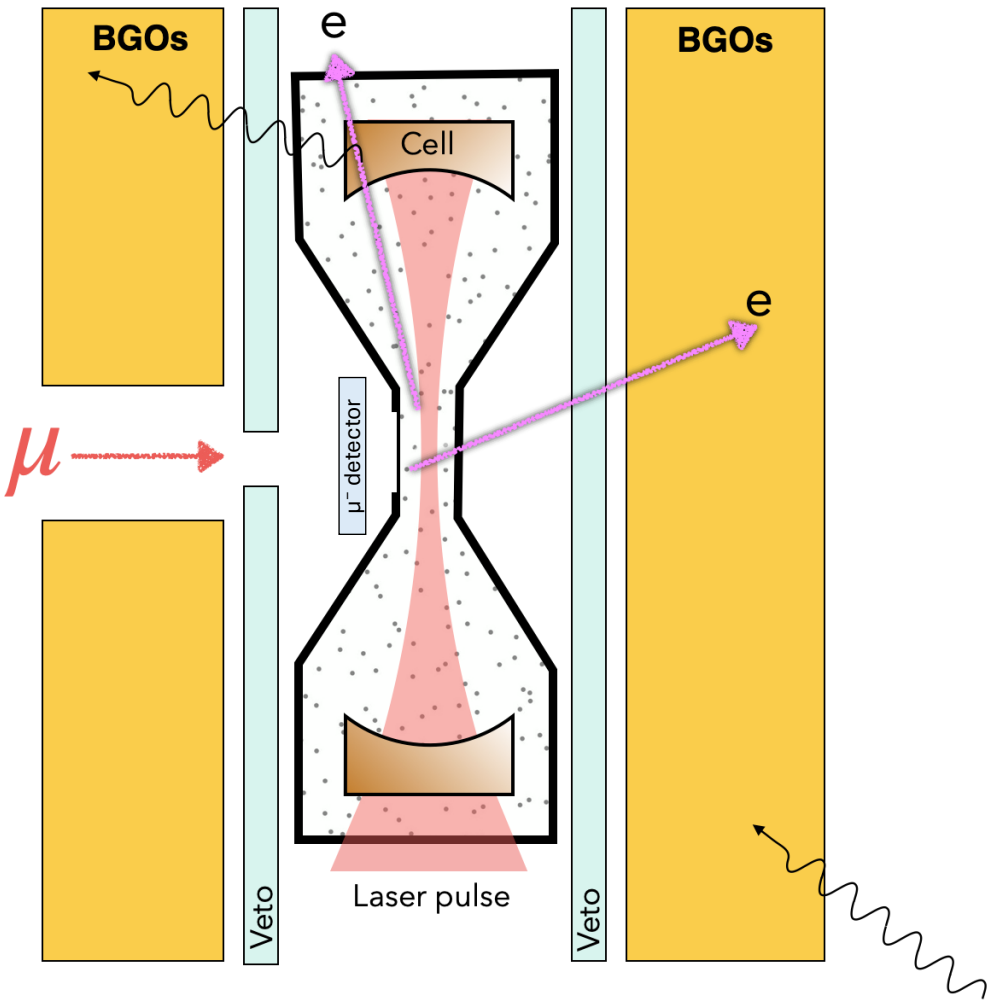

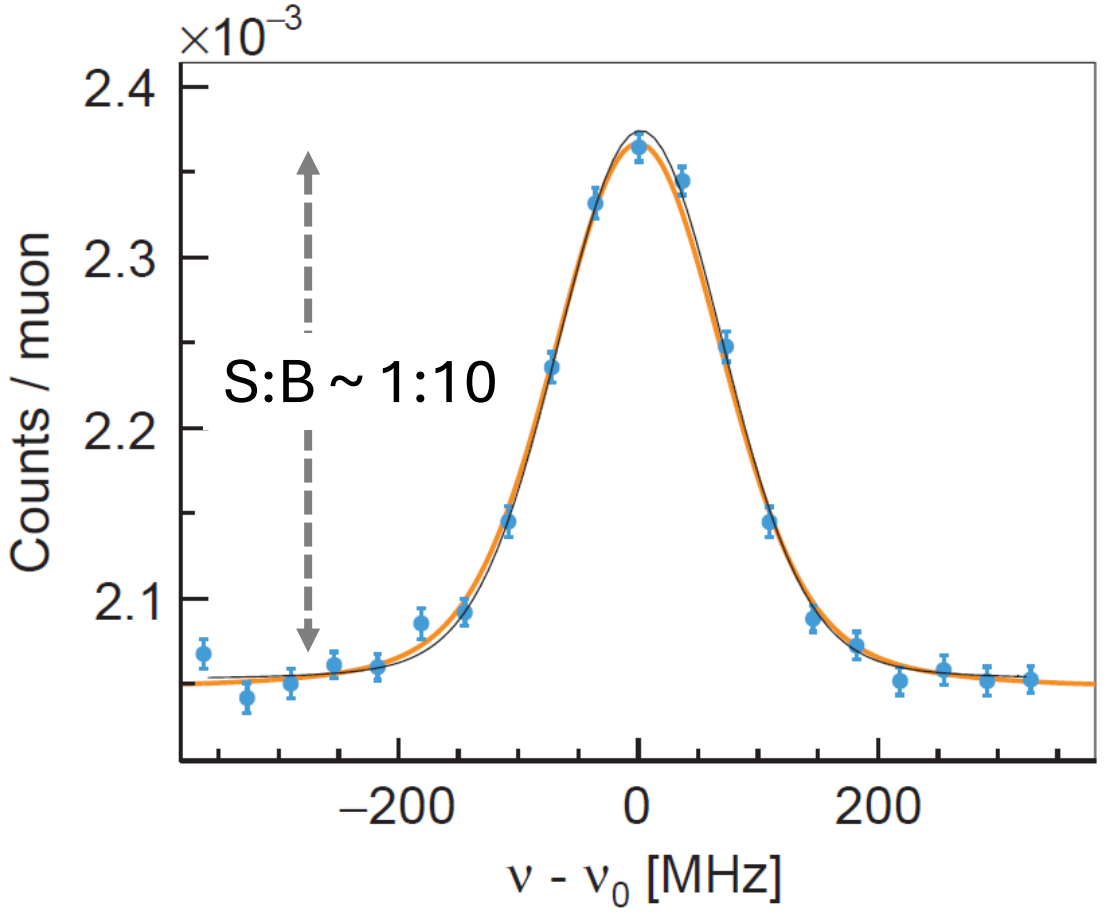

R_{signal}	:	$R_{\text{BG}}^{\text{diffusion}}$	:	$R_{\text{BG}}^{\text{decay}}$	:	$R_{\text{BG}}^{\text{accidental}}$
1		4.4		3.4		2.3

Nuber et al., SciPost Phys. Core 6, 057 (2023)

Signal and BG : Detection system prototype

$$\mu^- \xrightarrow[2.2\,\mu s]{} e^- + \bar{\nu}_e + \nu_\mu$$

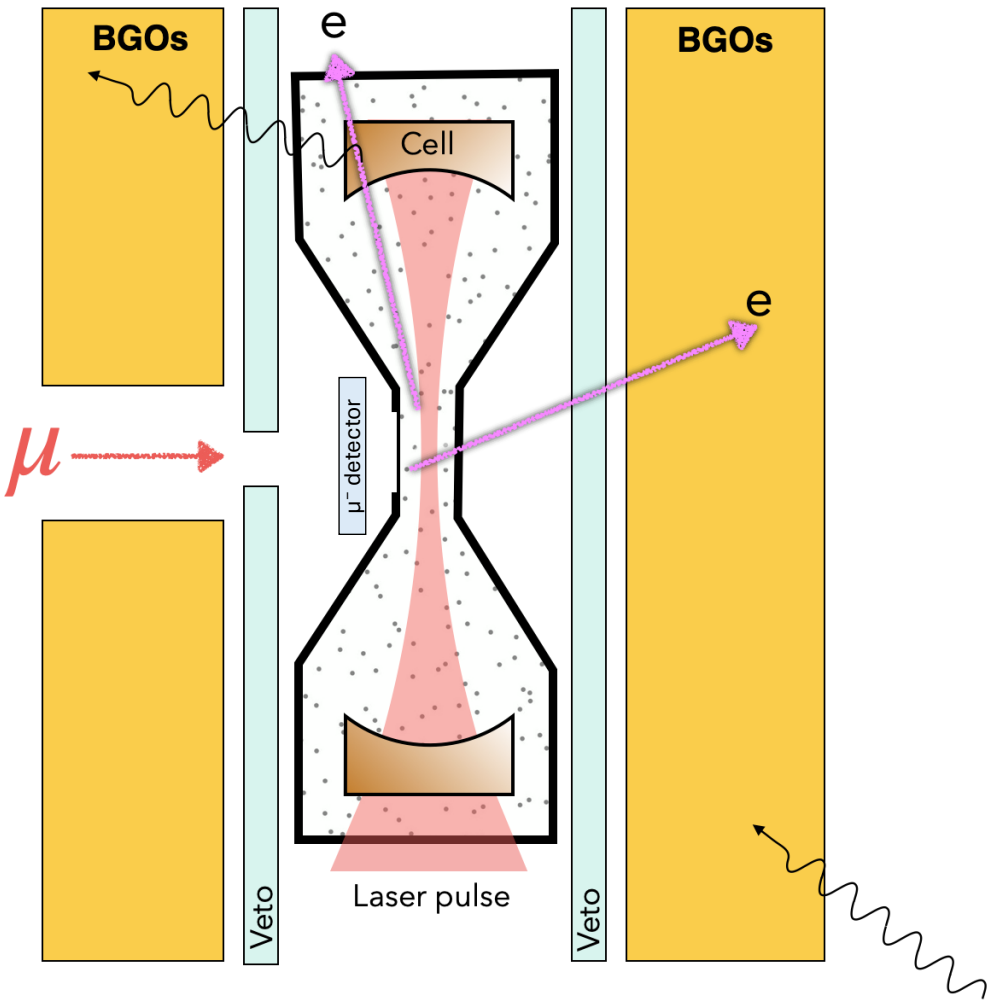

Nuber et al., SciPost Phys. Core 6, 057 (2023)

- Realistic material budget
- Measured detection probability
  - μAu event = 80%
  - false e^- iden. = 9%
- Fulfils requirements

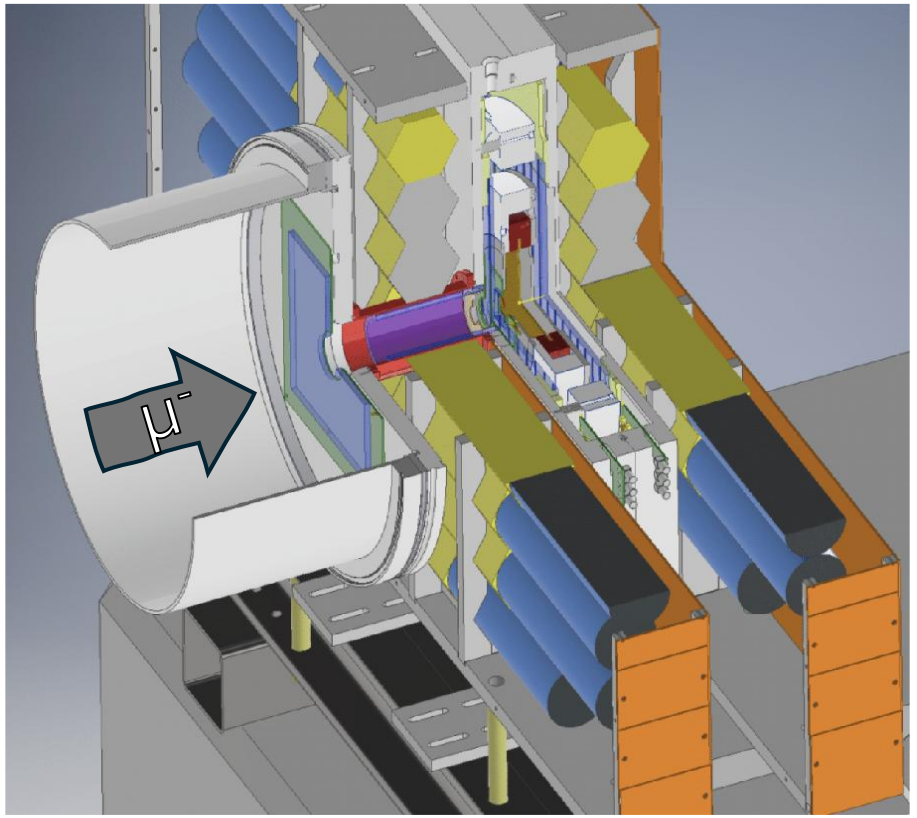

Signal and BG : Detection system prototype

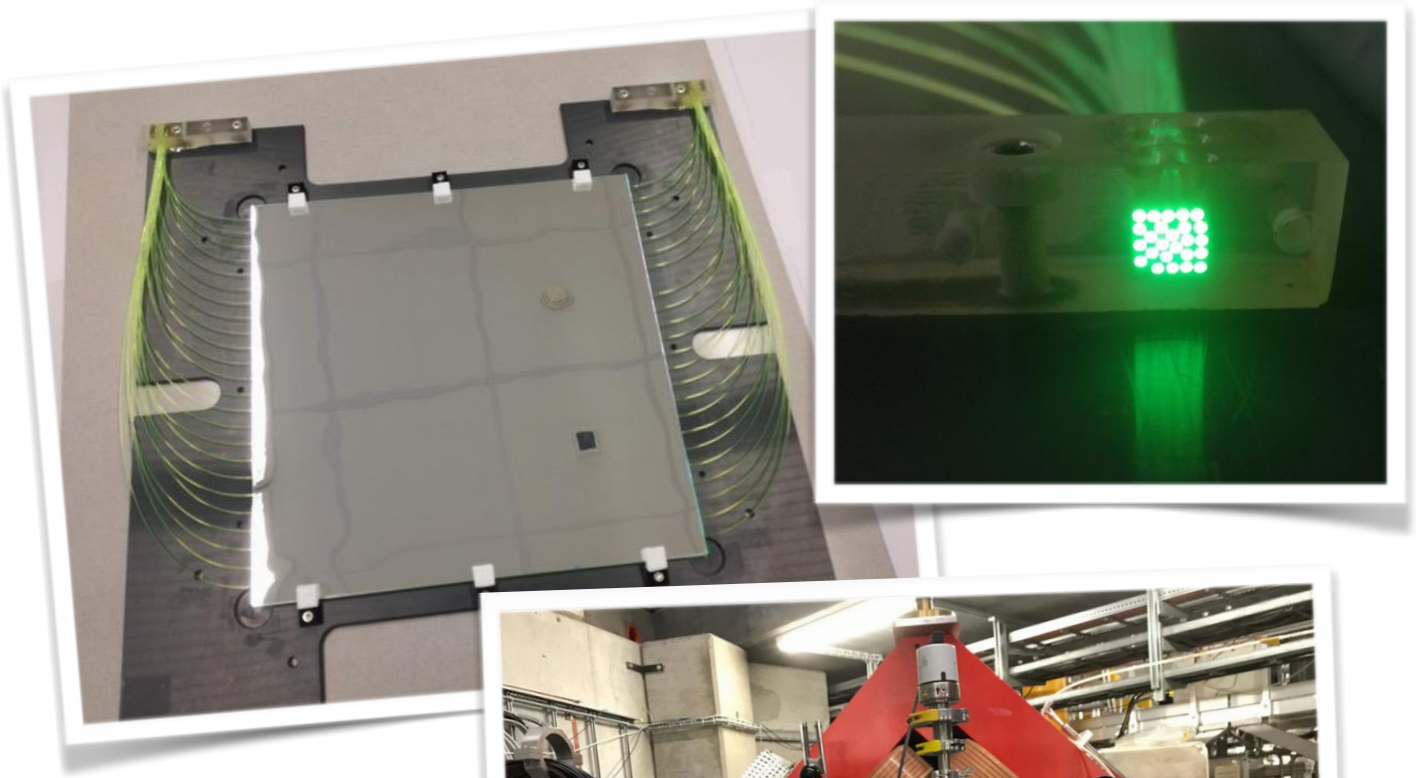

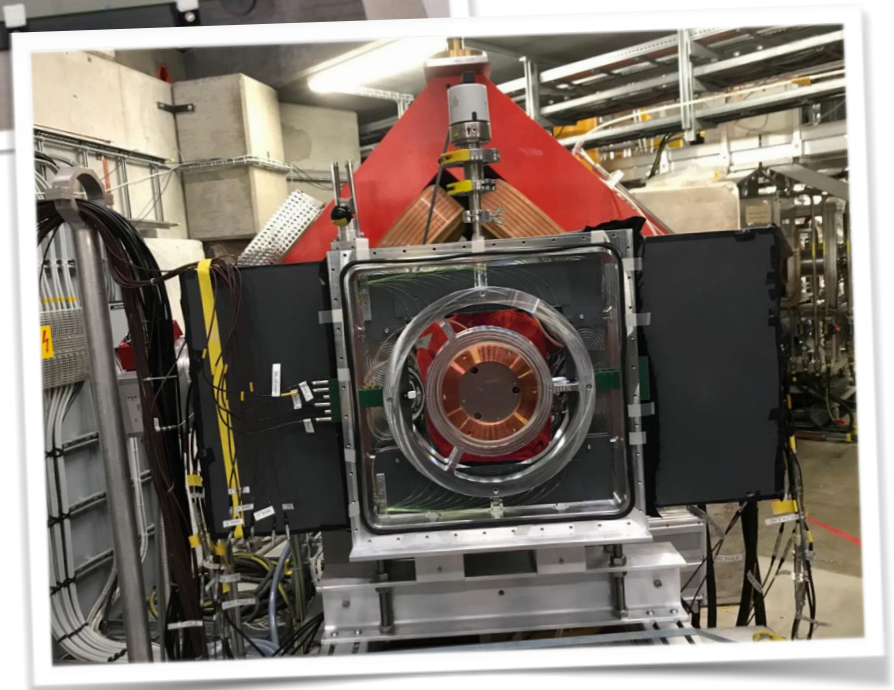

- Realistic material budget
- Measured detection probability
  - μAu event = 80%
  - false e^- iden. = 9%
- Fulfils requirements

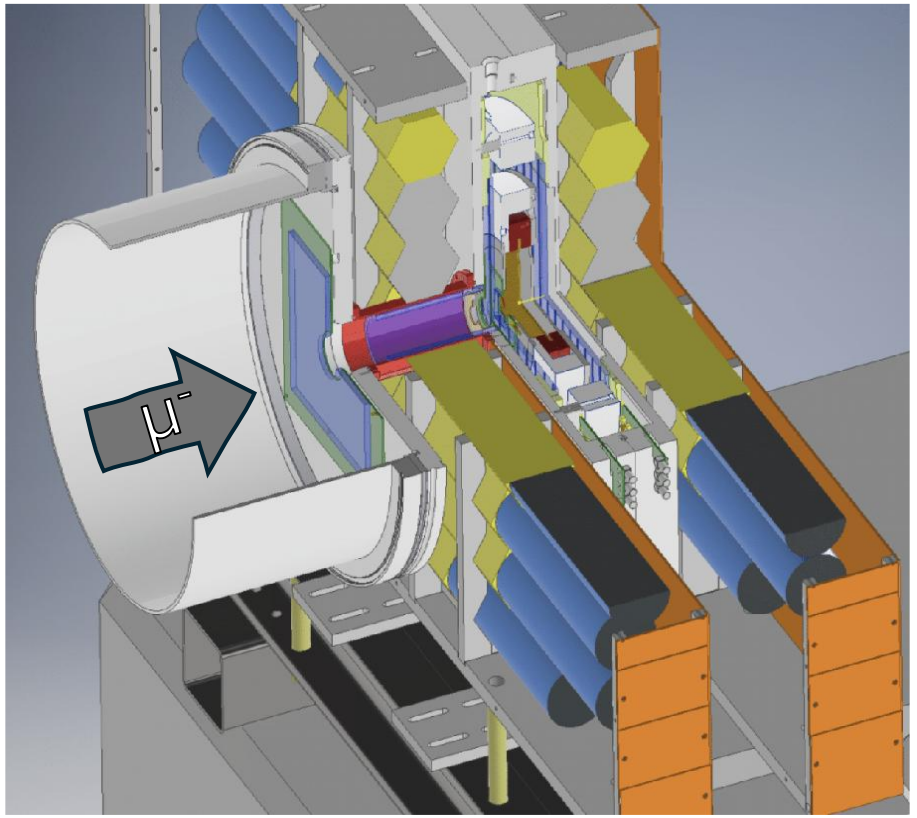

Hypermu-Beamtime

5 weeks of beamtime in PiE5 Nov-Dec 2026

Goals

- ☐ Full integration (μ^- beam, laser, enhancement cell, detector, cryogenic target….)
- ☐ Detector test for the first time in PiE5
- ☐ First diffusion data
- ☐ First resonance search attempt

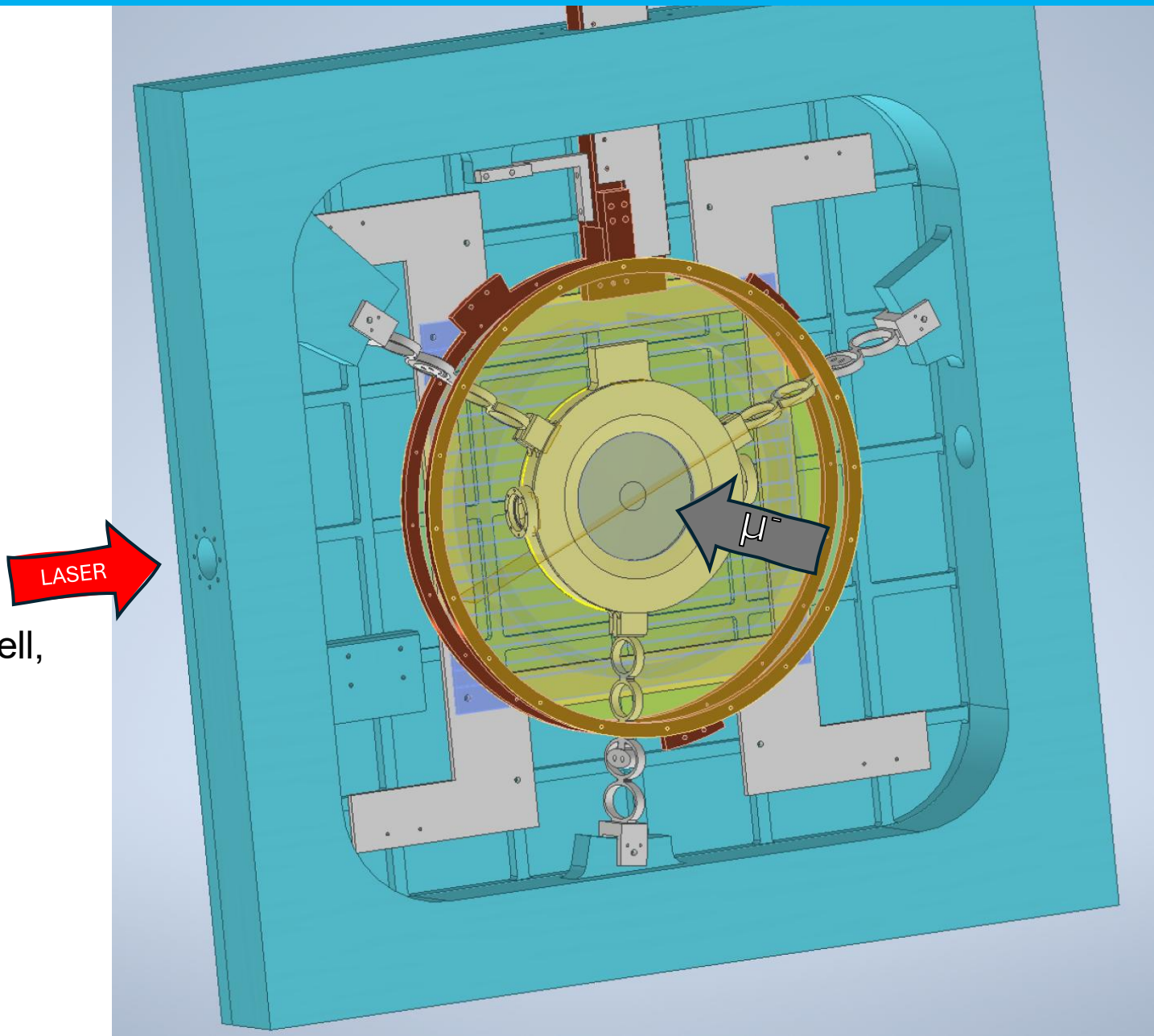

CREMA Collaboration

Laboratoire Kastler Brossel
Physique quantique et applications

P. Indelicato, F. Nez, N. Paul, P. Yzombard

MAX-PLANCK-INSTITUT FÜR QUANTENOPTIK GARCHING
MPQ

T.W. Hänsch

JG|U
JOHANNES GUTENBERG UNIVERSITÄT MAINZ

A. Ouf, R. Pohl, F. Wauters

國立清華大學
NATIONAL TSING HUA UNIVERSITY

Yi-Wei Liu, Tzu-Ling Chen

PSI ETH

L. Affoltern, D. Göldi, E. Gründeman, M. Kilinc, K. Kirch, F. Kottmann, D. Taqqu, A. Antognini, M. Hildebrandt, A. Knecht, S. Rajamohanan, A. Soter

UNIVERSIDADE NOVA DE LISBOA

P. Amaro, M. Ferro, M. Guerra, J. Machado, J. P. Santos,

IFJ PAN

A. Adamczak

IFSW
UNIVERSITÄT STUTTGART
INSTITUT FÜR STRAHLWERKZEUGE
STUTTGART LASER TECHNOLOGIES

M. Abdou-Ahmed, T. Graf

· U C ·
UNIVERSIDADE DE COIMBRA

F.D. Amaro, L.M.P. Fernandes, C. Henriques, C.M.B. Monteiro, J.M.F. dos Santos,